Cowles Foundation Discussion Papers   Cowles Foundation

Boosting the HP Filter for Trending Time Series with Long Range Dependence
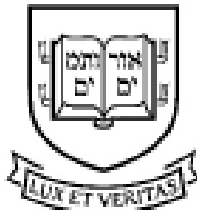
Eva Biswas

Farzad Sabzikar

Peter C. B. Phillips

BOOSTING THE HP FILTER FOR TRENDING TIME SERIES WITH LONG RANGE DEPENDENCE

By

Eva Biswas, Farzad Sabzikar, and Peter C. B. Phillips

August 2022

Boosting the HP Filter for Trending Time Series with Long Range Dependence[*]

Eva Biswas, Farzad Sabzikar
Department of Statistics, Iowa State University

Peter C. B. Phillips
Yale University, University of Auckland, University of Southampton,
Singapore Management University

August 26, 2022

Abstract

This paper extends recent asymptotic theory developed for the Hodrick Prescott (HP) filter and boosted HP (bHP) filter to long range dependent time series that have fractional Brownian motion (fBM) limit processes after suitable standardization. Under general conditions it is shown that the asymptotic form of the HP filter is a smooth curve, analogous to the finding in Phillips and Jin (2021) for integrated time series and series with deterministic drifts. Boosting the filter using the iterative procedure suggested in Phillips and Shi (2021) leads under well defined rate conditions to a consistent estimate of the fBM limit process or the fBM limit process with an accompanying deterministic drift when that is present. A stopping criterion is used to automate the boosting algorithm, giving a data-determined method for practical implementation. The theory is illustrated in simulations and two real data examples that highlight the differences between simple HP filtering and the use of boosting. The analysis is assisted by employing a uniformly and almost surely convergent trigonometric series representation of fBM.

Key words: Boosting, Brownian motion, fractional process, HP filter, long range dependence.

JEL codes C22, C55, E20

1 Introduction

Whittaker (1922) introduced a method of graduating (now commonly known as smoothing) data based on penalized maximum likelihood, minimizing an error sum of squares subject to a penalty

based on squares of third-order data differences to control roughness in the fitted curve. This method was justified in Whittaker and Robinson (1924) by a Bayesian approach that combined a Gaussian likelihood for the data with a Gaussian prior reflecting the presumed desirable property of smoothness. Following much earlier work by Leser (1961) designed specifically for economic time series applications and trend estimation, Hodrick and Prescott (1980, 1997) used second-order data differences in the penalty. This approach became influential in macroeconometric work and subsequently known as the 'HP filter'.[1]

Let $\{x_t\}_{t=1}^n$ be a time series with an unknown trend component f_t and stationary component c_t that may contain a regular cyclical component. Phillips and Jin (2021)(hereafter PJ) suggested a general form of Whittaker's smoothing filter to identify the long run trend f_t in x_t by solving the following constrained optimization problem

$$\hat{f}_t = \arg\min_{f_t} \left\{ \sum_{t=1}^n (x_t - f_t)^2 + \lambda \sum_{t=m+1}^n (\Delta^\delta f_t)^2 \right\}, \quad \text{with } \hat{c}_t = x_t - \hat{f}_t, \tag{1}$$

where $\lambda \geq 0$ is the smoothing parameter or tuning parameter, $\Delta = 1 - L$, L is the lag operator defined by $Lf_t = f_{t-1}$ and $\Delta^\delta f_t$ is the δth difference of f_t. The residual $\hat{c}_t$ is usually taken to provide an estimate of the business cycle in economic applications, following Hodrick and Prescott (1997). The first summation in (1) penalizes lack of fitness and the second summation penalizes lack of smoothness. The filter is one-sided for the first and the last δ number of observations and is two-sided for all the remaining observations. When $\delta = 2$, the procedure is the HP filter. The constrained optimization problem (1) involves a least squares fit coupled with an ℓ_2 norm penalty function. Recent work (Kim et al., 2009; Tibshirani, 2014; Yamada and Bao, 2021) has examined the use of an ℓ_1 norm penalty for trend filtering, which has the capability of capturing kinks in deterministic trends and producing piecewise linear trend estimates.

A key component of the filtering procedure (1) is the tuning parameter λ which controls the strength of the penalty in the optimization problem. Tuning parameters play an essential role in all types of nonparametric estimation and regression. These parameters influence smoothness, rate of convergence, and the orders of magnitude of the bias and variance. Likewise in filtering time series using (1), the choice of λ and its asymptotic behavior turns out to play an important role in determining the properties of trend functions estimated using the HP filter. Notably, as λ increases, the penalty for lack of smoothness rises forcing the estimate $\hat{f}_t$ to become smoother. When $\delta = 2$ second-order differences of a linear trend are 0, so that increasing λ makes $\hat{f}_t$ progressively linear, becoming a straight line as $\lambda \to \infty$. If the underlying trend process is actually nonlinear, then as λ rises the estimated trend $\hat{f}_t$ becomes so smooth that the estimated cycle $\hat{c}_t$ inherits some of the original features of the trend. On the other hand, if λ is small, the estimated trend $\hat{f}_t$ captures much of the fine grain features of the short-term movements in the data. In some cases, such as when the underlying trend is well-modeled by a random wandering stochastic process, separating the trend from cycle and noise is a serious challenge and choice of λ plays a major role in determining the properties and accuracy of the trend and implied cycle.

Understanding the large sample properties of filters such as $\hat{f}_t$ in (1) helps to meet this challenge by characterizing the various trend-capture capabilities of these filters as the sample size $n \to$

---

[1]Readers are referred to PJ(2021) for more detailed discussion and historical information on the filter.

∞. PJ (2021)[2] provided the first asymptotic analysis of the behavior of the HP filter, considering certain prototypical cases where suitably standardized data of the form $n^{-1/2}x_{t=\lfloor nr \rfloor}$ have stochastic process limits that involve Brownian motion. Three cases were considered, including a stochastic process with no deterministic drift, a stochastic process with a continuous drift function, and a stochastic process with a discrete number of trend breaks. For the case with no drift, they showed that if $\lambda = O(n^4)$ as $n \to \infty$ the estimated trend $n^{-1/2}\hat{f}_{t=\lfloor nr \rfloor}$ converges to a much smoother, four times differentiable stochastic process in place of Brownian motion. So the HP filter is inconsistent in this case. When a linear drift is present, the drift is consistently estimated by the HP filter but for more complex deterministic drifts or trend breaks the filter is inconsistent. In the presence of a trend break process, the limiting form of the estimated trend smooths over the trend break. In all these cases when $\lambda = O(n^4)$ the estimated cycle inherits some properties of the underlying stochastic trend. These asymptotic findings depend on the mutual relation between n and λ and, particularly, on the expansion rate of λ as $n \to \infty$. In general, faster expansion rates of λ yield smoother curves for the fitted trend function, whereas slower expansion rates captures more short-term fluctuations in the underlying stochastic process and deterministic drift function. Importantly, for sample sizes typical in applied macroeconomics, PJ (2021) found that the setting $\lambda = O(n^4)$ gave empirical results closely resembling those for the setting $\lambda = 1600$ commonly used in empirical work with quarterly aggregate data.

In related work, Phillips and Shi (2021)(hereafter PS) developed a boosting algorithm (Tukey, 1977; Buja et al., 1989) for the HP filter to address the inconsistency of the trend estimate with penalty setting $\lambda = O(n^4)$. This algorithm involves repeated use (m iterations) of the filter to refine the original estimate. Under certain conditions as $m \to \infty$ boosting the filter in this way provides successive refinements that lead to consistent estimates of the underlying trend and cycle. PS (2021) demonstrated the advantages of boosting in simulations and several empirical illustrations with economic data. They also developed data-determined selection procedures for choice of the number of boosting iterations in practical work.

The current paper seeks to extend the work of PJ(2021) and PS(2021) to a much wider class of stochastically nonstationary time series. In particular, we develop asymptotic theory for filtering trends that are generated by fractionally integrated time series using the HP filter. Suppose x_t is a fractionally integrated time series which has a fractional stochastic process limit upon suitable standardization such that $n^{-H}x_{\lfloor nr \rfloor} \rightsquigarrow B_H(r)$, where B_H is fractional Brownian motion (fBM) with Hurst parameter $H \in (0,1)$ and stationary increments that have long-range dependence, and $\rightsquigarrow$ signifies weak convergence. PJ(2021) and PS(2021) used the Karhunen-Loève orthonormal series representation of Brownian motion in developing the limit theory for HP and Whittaker filters when $H = 1/2$ and the time series satisfies $n^{-1/2}x_{\lfloor nr \rfloor} \rightsquigarrow B(r)$. This paper employs new orthonormal series representations suited to fBM to develop the limit theory of the filters. The results developed here include those for the special case of an integrated process with a Brownian motion limit.

The paper is organized as follows. Section 2 provides some essential properties of stochastic processes with long-range dependence that are used later in the paper. Section 3 shows that when the data are fractionally integrated and satisfy $n^{-H}x_{\lfloor nr \rfloor} \rightsquigarrow B_H(r)$ the HP filter trend estimate obtained with the tuning parameter setting $\lambda = O(n^4)$ is inconsistent and instead delivers a limit

---

[2]The original version of this paper which developed asymptotic theory for the HP filter was circulated as a working paper in Phillips and Jin (2002).

that is a smoothed version of the underlying trend process $B_H(r)$, analogous to the result of PJ (2021) for $I(1)$ integrated processes. Section 4 provides extensions of this finding to more general trends, giving conditions for the consistent estimation of the trend by the boosted HP (bHP) filter for fractional processes, fractional processes with polynomial and continuous drift functions as well as trending data with trend breaks. Section 5 reports simulations demonstrating finite sample performance of the filters in relation to the asymptotic theory, gives a stopping time rule for practical implementation, and provides a brief empirical application of the methodology. Sections 7 and 8 are appendices with proofs (Appendix A) and useful strong approximation results (Appendix B), respectively.

2 Long-Range Dependence

This section briefly overviews some essential definitions and results related to time series with different covariance structures, including long-range dependence (LRD) and negative memory (antipersistence), and their limit processes used in the rest of the paper.

A covariance stationary time series $\{u_t^z\}_{t\in\mathbb{Z}}$ with autocovariance $\gamma_u(k) = \mathbb{E}(u_t^z u_{t+h}^z)$ is said to have LRD if $\sum_{k\in\mathbb{Z}} |\gamma_u(k)| = \infty$. A commonly used class of LRD time series is the fractionally integrated class, denoted $I(d^*)$, with moving average representation

$$u_j^z = \sum_{k=0}^{\infty} a_k \varepsilon_{j-k}, \tag{2}$$

where $a_k \sim \frac{c_a}{k^{1-d^*}}$ as $k \to \infty$, with $c_a \neq 0$, $0 < d^* < 1/2$, and $\varepsilon_j \overset{iid}{\sim} (0,1)$. It can be shown (Giraitis et al., 2012, Proposition 3.2.1) that $\gamma_u(k) \sim \frac{c_\gamma}{k^{1-2d^*}}$, as $k \to \infty$, with $c_\gamma = c_a^2 \mathcal{B}(d^*, 1-2d^*)$ where $\mathcal{B}(\cdot,\cdot)$ is the beta function, from which it follows that $\sum_{k=0}^{\infty} |\gamma_u(k)| = \infty$. The covariance stationary time series $\{u_t^z\}_{t\in\mathbb{Z}}$ with autocovariance $\gamma_u(k) = \mathbb{E}(u_t^z u_{t+h}^z)$ is said to have negative memory, or antipersistence, if $\sum_{k=0}^{\infty} |\gamma_u(k)| < \infty$ and $\sum_{k=0}^{\infty} \gamma_u(k) = 0$. An empirically important special class of time series with negative memory is the $I(d^*)$ time series with the moving average representation (2) where $-1/2 < d^* < 0$ and $\sum_{k=0}^{\infty} a_k = 0$. The same proposition in Giraitis et al. (2012) shows that in this antipersistence case $\sum_{k\in\mathbb{Z}} \gamma_u(k) = 0$ and $\gamma_u(k) \sim \frac{c_\gamma}{|k|^{1-2d^*}}$, as $k \to \infty$, which means that $\sum_{k=0}^{\infty} |\gamma_u(k)| < \infty$ when $d^* \in (-1/2, 0)$.

Fractional Brownian motion (fBM) is a stochastic process with the moving average representation

$$B_H(t) = \frac{1}{A(H)} \left[\int_{-\infty}^{0} [(t-s)^{H-1/2} - (-s)^{H-1/2}] dB(s) + \int_{0}^{t} (t-s)^{H-1/2} dB(s) \right], \tag{3}$$

and covariance kernel

$$r_H(s,t) = \mathbb{E}\left(B_H(s) B_H(t)\right) = \frac{1}{2}\{|s|^{2H} + |t|^{2H} - |s-t|^{2H}\}, \quad t, s \in \mathbb{R}, \tag{4}$$

where $B(\cdot)$ is standard Brownian motion, $H \in (0,1)$, and

$$A(H) = \left(\frac{1}{2H} + \int_{0}^{\infty} [(1+s)^{H-1/2} - s^{H-1/2}]^2 ds \right)^{1/2}.$$

The increments of fBM form a stationary process with LRD when $1/2 < H < 1$ (Taqqu and Samorodnitsky, 1996, Proposition 7.2.10). We start our analysis by assuming $H \in (1/2, 1)$.

Let us define, z_t an $I(d)$ process with $d = d^* + 1$ by the following equation

$$z_t = \sum_{k=1}^{t} u_k^z \tag{5}$$

The next two results present useful connections between the $I(d)$ time series z_t and a limiting fBM process B_H with $H = d - 1/2$.

Lemma 2.1. *(Giraitis et al., 2012, Corollary 4.4.1) Let z_j be an $I(d)$ process given by (5) with $1 < d < 1.5$ and $H = d - 1/2$. Then, as $N \to \infty$,*

$$\frac{1}{N^{d-1/2}} z_{\lfloor Nt \rfloor} \rightsquigarrow s_d B_H(t),$$

in the Skorokhod space $\mathcal{D}[0, 1]$ with the uniform metric and where $s_d^2 = c_a^2 \frac{B(d-1, 3-2d)}{(d-1)(2d-1)}$.

Lemma 2.2. *(Wang et al., 2003, Corollary 1.1.) Let z_j be an $I(d)$ process as in (5). Then on an appropriate probability space for $\{\varepsilon_k\}$, we can construct a fractional Brownian motion $\{B_H(t)\}_{t \geq 0}$ with $H = d - 1/2$ such that*[3]

$$\sup_{0 \leq t \leq 1} \left| \frac{1}{c_a \kappa_H} z_{\lfloor Nt \rfloor} - B_H(Nt) \right| = o_{a.s.}(N^H (\log \log N)^{1/2}), \tag{6}$$

where $c_H = \int_0^\infty x^{H-3/2}(x+1)^{H-3/2} dx$ and $\kappa^2(H) = c_H(H - 1/2)^{-1}(2H)^{-1}$. If in addition $\mathbb{E}|\varepsilon_0|^p < \infty$ for some $p > 2$, then the term $o_{a.s.}(\cdot)$ on the right hand of (6) may be replaced by $o_{a.s.}(N^{H-1/2+1/p})$. Consequently,

$$\sup_{0 \leq t \leq 1} \left| \frac{1}{c_a \kappa_H} z_{\lfloor Nt \rfloor} - B_H(Nt) \right| = o_{a.s.}(N^{H-1/2+1/p}). \tag{7}$$

From the definition of fBM in (3), we have the self similarity

$$B_H(Nt) \triangleq N^H B_H(t), \tag{8}$$

where $\triangleq$ means equality in the sense of finite dimensional distributions. Using (7) and (8) gives

$$\sup_{0 \leq t \leq 1} \left| \frac{1}{c_a \kappa_H} \frac{z_{\lfloor Nt \rfloor}}{N^H} - B_H(t) \right| = o_{a.s.}(N^{\frac{1}{p} - \frac{1}{2}}), \tag{9}$$

provided $\mathbb{E}|\varepsilon_0|^p < \infty$ for some $p > 2$.

Lemma 2.2 provides a strong approximation for fBM with Hurst parameter $H \in (1/2, 1)$ leading to (9). The domain of strong approximation of fBM can be extended to the wider region $H \in (0, 1)$ using an approach developed by Szabados (2001) who constructed a stochastic process

---

[3]Correspondence with the notation in (Wang et al., 2003, Corollary 1.1.) involves setting their $\alpha = \frac{3}{2} - H$ and replacing their κ_α with our $c_a \kappa_H$ to accommodate the replacement of their moving average coefficients $\psi_k \sim_a k^{-\alpha}$ with our moving average coefficients $a_k \sim_a \frac{c_a}{k^{2-d}}$ where $d = H + 1/2$.

that converges to fBM with $H \in (0,1)$ using simple moving averages of a random walk. Details of this construction are provided in Appendix B. This work, like much of the discussion above, deals with what are generally known as Type I fBM processes - see (Marinucci and Robinson, 1999; Davidson and Hashimzade, 2009; Phillips, 2022). In nonstationary long memory time series, it is often convenient to work instead with a Type II fBM process

$$W_H(t) = \frac{1}{\Gamma(H+1/2)} \int_0^t (t-s)^{H-1/2} dB(s), \tag{10}$$

where $H > 0$. More specifically, consider the nonstationary fractional time series generated as

$$\tilde{z}_t = \sum_{j=0}^{t} \frac{(d)_j}{j!} \tilde{\varepsilon}_{t-j}, \tag{11}$$

where $d > 1/2$, $(d)_j = d(d+1)\cdots(d+j-1)$ is the forward factorial, and $\tilde{\varepsilon}_t$ is a zero mean short memory process with moments of high enough order and a suitable summability condition for its autocovariances. The following Lemma gives the asymptotic connection between a suitably normalized form of the time series $\tilde{z}_t$ and the Type II fBM process W_H with $H = d - 1/2$.

Lemma 2.3. *(Phillips, 2022, Lemma 4.7) Let $\tilde{z}_j$ be a long memory time series generated by* (11) *with $d > 1/2$ and $\tilde{\varepsilon}_j \overset{iid}{\sim} (0,1)$ with $\mathbb{E}|\tilde{\varepsilon}_j|^p < \infty$ for some $p > \max\left(\frac{1}{d-1/2}, 2\right)$. Then, as $N \to \infty$,*

$$\frac{1}{N^{d-1/2}} \tilde{z}_{\lfloor Nt \rfloor} \rightsquigarrow W_H(t), \tag{12}$$

where W_H is the Type II fBM given by (10) *with $H = d - 1/2$.*

With a suitable extension of the probability space the weak convergence in (12) can be replaced by $a.s.$ convergence.

The following result gives a useful orthonormal series representation of B_H due to Dzhaparidze and Van Zanten (2004, Theorem 4.5).

Theorem 2.4. *For any $H \in (0,1)$ let $u_1 < u_2 < \cdots$ be the positive real zeros of J_{-H} and $v_1 < v_2 < \cdots$ be the positive real zeros of $J_{1-H}(z)$, where J_ν is a Bessel function*[4] *of the first kind of order ν. Assume $\{U_k\}_{k=1}^\infty$ and $\{V_k\}_{k=1}^\infty$ are independent Gaussian random variables with mean zero and variances*

$$Var(U_k) = 2C_H^2 u_k^{-2H} J_{1-H}^{-2}(u_k), Var(V_k) = 2C_H^2 v_k^{-2H} J_{-H}^{-2}(v_k), C_H^2 = \pi^{-1}\Gamma(1+2H)\sin \pi H. \tag{13}$$

Then a standard fBM $B_H(r)$ over $r \in [0,1]$ can be represented $a.s.$ in terms of the series

$$B_H(r) = \sum_{k=1}^\infty \frac{\sin u_k r}{u_k} U_k + \sum_{k=1}^\infty \frac{1 - \cos v_k r}{v_k} V_k, \tag{14}$$

both series converging absolutely, and uniformly in $r \in [0,1]$ with probability 1.

---

[4]In hypergeometric series form $J_\nu(z) = \frac{(\frac{z}{2})^\alpha}{\Gamma(\alpha+1)} {}_0F_1\left(\alpha+1; -\left(\frac{z}{2}\right)^2\right) = \sum_{k=0}^\infty \frac{(-1)^n (z/2)^{\nu+2k}}{\Gamma(k+1)\Gamma(\nu+k+1)}$, where $\Gamma(z)$ is the gamma function and ${}_0F_1(\cdot;\cdot)$ the $(0,1)$ hypergeometric series.

When $H = 1/2$ we have $c_{1/2} = 1/\pi$ and the series representation (14) reduces to the following orthonormal series representation of standard Brownian motion

$$B(r) = \sum_{k=1}^{\infty} \frac{\sin((k - \frac{1}{2})\pi r)}{(k - \frac{1}{2})\pi} U_k' + \sum_{k=1}^{\infty} \frac{1 - \cos(k\pi r)}{k\pi} V_k', \tag{15}$$

which is an alternative representation to the Karhunen-Loève series $B(r) = \sqrt{2} \sum_{k=1}^{\infty} \frac{\sin((k - \frac{1}{2})\pi r)}{(k - \frac{1}{2})\pi} U_k'$. Here U_k' and V_k' follows standard normal distribution.

3 Asymptotic Theory of the HP filter

The HP filter is a practical technique designed to separate time series data $(x_t : t = 1, \cdots, n)$ into an underlying trend component f_t and a residual cycle c_t. Assuming $x_t = f_t + c_t$, the filter computes estimates of f_t and c_t by solving

$$\hat{f}_t = \arg\min \left\{ \sum_{t=1}^{n} (x_t - f_t)^2 + \lambda \sum_{t=3}^{n} (\Delta^2 f_t)^2 \right\}, \quad \hat{c}_t = x_t - \hat{f}_t, \tag{16}$$

where $\lambda > 0$ is the tuning parameter that controls data smoothing, $\Delta = 1 - L$, L is the lag operator defined by $Lf_t = f_{t-1}$ and $\Delta^2 f_t$ is the 2nd order difference of f_t. The first term of (16) penalizes the lack of fitness and the second term penalizes lack of smoothness. The filter is one sided for the first 2 and the final 2 observations and two sided for the remaining observations.

In solution matrix form, the estimated trend vector $\hat{f}^{HP} = (\hat{f}_1^{HP}, ..., \hat{f}_n^{HP})'$ is given by

$$\hat{f}^{HP} = (I + \lambda D_2 D_2')^{-1} x, \tag{17}$$

where $x = (x_1, ..., x_n)'$ and D_2' is the rectangular $(n-2) \times n$ block matrix $D_2' = \text{diag}\{d_2', d_2', ..., d_2'\}$ with $d_2' = (1, -2, 1)$. Neglecting the first 2 and final 2 rows of (17), the solution can be written in operator form as[5]

$$\hat{f}_t^{HP} = [\lambda L^{-2}(1 - L)^4 + 1]^{-1} x_t, \quad \hat{c}_t^{HP} = \frac{\lambda L^{-2}(1 - L)^4}{1 + \lambda L^{-2}(1 - L)^4} x_t. \tag{18}$$

These operator forms of $\hat{f}_t^{HP}$ and $\hat{c}_t^{HP}$ are particularly useful in developing asymptotic theory for the filter as the sample size $n \to \infty$ and they will be used through the rest of this paper. In developing an asymptotic theory for the HP filter PJ(2021) obtained large sample representations of the operator forms in (18) for the case where the standardized data process $\frac{x_{t=\lfloor n \cdot \rfloor}}{\sqrt{n}}$ converges as $n \to \infty$ to Brownian motion or Brownian motion with general drift functions and possible breaks. That limit theory allowed for different scenarios concerning the behavior of the tuning parameter λ. When $\lambda = O(n^4)$, the estimated trend function was shown to be inconsistent, converging instead to a limiting stochastic process smoother than Brownian motion; but when $\lambda = o(n)$ the estimated trend function is consistent and converges to Brownian motion. Small values or low expansion rates

---

[5]See PJ(2021) for more details, including exact finite sample operator representations of the HP and more general versions of the Whittaker filter.

of λ relative to the sample size naturally tend to capture more granular movement in the underlying process, thereby reproducing the series itself rather than separating out more slow moving trend processes. The present development extends this asymptotic analysis to cases involving time series with long range dependence that, upon suitable normalization, have limiting fBM stochastic process forms.

Recall the $I(d)$ process $\{z_j\}$ satisfying the conditions of Lemmas 2.1 and 2.2. Hence $x_t := \frac{1}{c_a \kappa_H} \sum_{j=1}^{t} u_t^z = \frac{1}{c_a \kappa_H} z_t$ follows the functional law-

$$X_n(\cdot) := \frac{x_{t=\lfloor n \cdot \rfloor}}{n^H} \rightsquigarrow B_H(\cdot), \tag{19}$$

where B_H is fBM given by (3). Further, from (9), we have the strong approximation

$$\sup_{0 \le t \le n} \left| \frac{x_t}{n^H} - B_H\left(\frac{t}{n}\right) \right| = o_{a.s.}\left(\frac{1}{n^{1/2-1/p}}\right), \quad \text{for } H \in (1/2, 1), \tag{20}$$

provided $\mathbb{E}|\varepsilon_0|^p < \infty$ for some $p > 2$. Thus, on a suitably extended probability space we have

$$\frac{x_{\lfloor nr \rfloor}}{n^H} - B_H(r) = o_{a.s.}(1), \text{ for } H \in (1/2, 1). \tag{21}$$

This strong approximation can be further extended to hold over the wider range $H \in (0,1)$ using the alternative constructive approach developed by Szabados (2001), as mentioned above and discussed in Appendix B.

To proceed with the extension of the asymptotic analysis of the HP filter to the fractional process case we make the following assumptions.

Assumptions:

(A) Upon normalization by n^H for some $H \in (0,1)$, the time series x_t satisfies

$$\frac{x_{\lfloor nr \rfloor}}{n^H} \rightsquigarrow B_H(r), \ r \in [0,1], \tag{22}$$

and in a suitably expanded probability space $\frac{x_{\lfloor nr \rfloor}}{n^H} \xrightarrow{a.s.} B_H(r)$.

(B) Corresponding to (A), the true trend function f_t is assumed to have an asymptotic trend form in the same normalized space. In particular, the normalized trend can be represented as $n^{-H} f_t = F_n\left(\frac{t}{n}\right)$, where F_n is a continuous function which interpolates the points $\{n^{-H} f_t : t = 1, 2, \cdots, n\}$, and as $n \to \infty$

$$\frac{f_{t=\lfloor nr \rfloor}}{n^H} = F_n\left(\frac{\lfloor nr \rfloor}{n}\right) \rightsquigarrow f(r), \tag{23}$$

for some continuous (possibly stochastic) limiting trend function $f(r)$. Further, with an appropriate extension of the probability space

$$\frac{f_{\lfloor nr \rfloor}}{n^H} - f(r) = o_{a.s.}(1). \tag{24}$$

In the following result we set the tuning parameter to be $\lambda = \mu n^4$. PJ(2021) found that this setting gave results for the HP filter similar to those commonly obtained in empirical work with sample sizes of the magnitude common in applied macroeconomic data.

Theorem 3.1. *Let x_t satisfy the functional law* (22) *and $\lambda = \mu n^4$. For $r \in [0,1]$ define*

$$G_l^H(r) = \sum_{k=1}^{l} \frac{1}{\mu u_k^4 + 1} \frac{\sin u_k r}{u_k} U_k + \sum_{k=1}^{l} \left(\frac{1}{v_k} - \frac{1}{\mu v_k^4 + 1} \frac{\cos v_k r}{v_k} \right) V_k \tag{25}$$

and

$$G_\infty^H(r) = \sum_{k=1}^{\infty} \frac{1}{\mu u_k^4 + 1} \frac{\sin u_k r}{u_k} U_k + \sum_{k=1}^{\infty} \left(\frac{1}{v_k} - \frac{1}{\mu v_k^4 + 1} \frac{\cos v_k r}{v_k} \right) V_k, \tag{26}$$

where $\{U_i\}_{i=1}^{\infty}$ and $\{V_i\}_{i=1}^{\infty}$ are independent Gaussian random variables with zero means and variances given by (13). *Then*

(i) *$G_l^H(\cdot)$ converges to the Gaussian process $G_\infty^H(\cdot)$ uniformly for $r \in (0,1)$ and $H \in (0,1)$ as $l \to \infty$.*

(ii) *If the HP filter is applied to x_t and in the expanded probability space where $\frac{x_{\lfloor nr \rfloor}}{n^H} \xrightarrow{a.s.} B_H(r)$ and* (24) *holds, the estimated trend $\hat{f}_{t=\lfloor nr \rfloor}^{\mathrm{HP}}$ has the following limiting form for $H \in (0,1)$ as $n \to \infty$*

$$\frac{\hat{f}_{\lfloor nr \rfloor}^{\mathrm{HP}}}{n^H} \xrightarrow{a.s.} G_\infty^H(r), \tag{27}$$

and

$$\left| \frac{\hat{f}_{\lfloor nr \rfloor}^{\mathrm{HP}}}{n^H} - G_{K_n}^H(r) \right| \xrightarrow{a.s.} 0. \tag{28}$$

provided $\frac{K_n}{n} \to 0$ as $n, K_n \to \infty$.

Remarks 3.2. *Theorem 3.1 shows that if x_t is an $I(d)$ process with $d \in (1, 1.5)$ given by the normalized partial sum process $x_t = \frac{1}{c_a \kappa_H} \sum_{j=1}^{t} u_j^z$, as in the functional law convergence* (19), *and satisfying* (21) *on the suitably expanded probability space, then the limit theory for the HP filter trend estimate $\hat{f}_t^{\mathrm{HP}}$ can be expressed as $n^{-H} \hat{f}_{\lfloor nr \rfloor}^{\mathrm{HP}} \xrightarrow{a.s.} G_\infty^H(r)$ for $H \in (\frac{1}{2}, 1)$ and $r \in (0,1)$. The result is extended to $H \in (0,1)$ using the construction and strong approximation of Szabados (2001).*

Remarks 3.3. *The Gaussian process $G_\infty^H(\cdot)$ defined by* (26) *is continuous and four times differentiable on $[0,1]$. To see this, define $G_{\infty,1}(r) = \sum_{k=1}^{\infty} \frac{1}{\mu u_k^4 + 1} \frac{\sin u_k r}{u_k} U_k$ and $G_{\infty,2}(r) = \sum_{k=1}^{\infty} \frac{1}{\mu v_k^4 + 1} \frac{\cos v_k r}{v_k} V_k$. Note that*

$$\frac{1}{h} \left[\frac{1}{\mu u_k^4 + 1} \frac{\sin u_k (r+h)}{u_k} U_k - \frac{1}{\mu u_k^4 + 1} \frac{\sin u_k r}{u_k} U_k \right] = \frac{U_k}{\mu u_k^4 + 1} \frac{2 \cos \frac{u_k(2r+h)}{2} \sin \frac{u_k h}{2}}{h u_k}$$

$$\to \frac{U_k}{\mu u_k^4 + 1} \cos u_k r, \quad as \ h \to 0.$$

Since $\sum_{k=1}^{\infty} \frac{U_k}{\mu u_k^4 + 1} \cos u_k r < \infty$ (see the proof of 3.1), it follows that $G_{\infty,1}(r)$ is differentiable. In a similar fashion, $G_{\infty,2}(r)$ is differentiable. The quantitities $\frac{V_k}{v_k}$ are independent of r for all $k \in \mathbb{Z}^+$. Hence G_∞^H is differentiable. Repeating this process, it can be shown that G_∞^H is four times continuously differentiable by using the fact that $\sum_{k=1}^{\infty} \frac{U_k}{u_k^{1+\delta}} < \infty$ and $\sum_{k=1}^{\infty} \frac{V_k}{v_k^{1+\delta}} < \infty$ for all $\delta \geq 0$. It follows that the limit of the HP estimated trend function is a smooth four-times differentiable Gaussian process distinct from the fBM limit $B_H(r)$, which is a continuous non-differentiable process.

Remarks 3.4. *Evidently the HP filter does not produce a consistent estimate of the trend when the underlying time series x_t satisfies the functional law (22). The cyclical residual of the HP filter is $\hat{c}_t = x_t - \hat{f}_t$. Suitably normalized and in the expanded probability space, this residual satisfies*

$$\frac{\hat{c}_{t=\lfloor nr \rfloor}}{n^H} = \frac{x_{\lfloor nr \rfloor}}{n^H} - \frac{\hat{f}_{\lfloor nr \rfloor}}{n^H} \rightarrow_{a.s.} \sum_{k=1}^{\infty} \frac{\mu u_k^4}{\mu u_k^4 + 1} \frac{\sin u_k r}{u_k} U_k - \sum_{k=1}^{\infty} \left(\frac{1}{v_k} - \frac{1}{\mu v_k^4 + 1} \frac{\cos v_k r}{v_k} \right) V_k.$$

The limiting stochastic process $\sum_{k=1}^{\infty} \frac{\mu u_k^4}{\mu u_k^4 + 1} \frac{\sin u_k r}{u_k} U_k$ of the HP residual $\frac{\hat{c}_{\lfloor nr \rfloor}}{n^H}$ is continuous but not differentiable, thereby inheriting one of the distinctive properties of the underlying fBM trend function $B_H(r)$. It follows that the HP filter fails to completely detrend the stochastic process and instead smooths that trend process into a differentiable limit function. The result is entirely analogous to the Brownian motion limit case where $H = 1/2$ studied in PJ(2021).

Remarks 3.5. *To obtain a consistent trend estimator by means of the HP filter one approach is to lower the expansion rate of the tuning parameter from $\lambda = O(n^4)$. This can be achieved by letting the scale parameter $\mu = \mu_l$ depend on a sequence $l \to \infty$ with the property that $\mu_l \to 0$. If sequential limits are taken with $n \to \infty$ followed by $l \to \infty$, which is represented by $(l,n)_{seq} \to \infty$, then it is apparent from the limit theory (26) in theorem 3.1 that*

$$\frac{\hat{f}_{\lfloor nr \rfloor}^{\text{HP}}}{n^H} \xrightarrow[n\to\infty]{a.s.} G_\infty^H(r) = \sum_{k=1}^{\infty} \frac{1}{\mu_l u_k^4 + 1} \frac{\sin u_k r}{u_k} U_k + \sum_{k=1}^{\infty} \left(\frac{1}{v_k} - \frac{1}{\mu_l v_k^4 + 1} \frac{\cos v_k r}{v_k} \right) V_k$$

$$\xrightarrow[l\to\infty]{a.s.} \sum_{k=1}^{\infty} \frac{\sin u_k r}{u_k} U_k + \sum_{k=1}^{\infty} \frac{1 - \cos v_k r}{v_k} V_k = B_H(r), \tag{29}$$

in view of the series representation (14) given in Theorem 2.4. The sequential convergence (29) suggests that the underlying fBM trend can be obtained asymptotically by lowering the expansion rate of λ. PJ(2021) showed that in the Brownian motion case ($H = 1/2$) this is achieved by setting $\lambda \to \infty$ as $n \to \infty$ such that $\lambda = o(n)$. The same property holds in the present case.

Remarks 3.6. *Theorem 3.1 in PJ (2021) shows that when x_t is an $I(1)$ integrated process, corresponding to $H = 1/2$, the standardized HP filter $n^{-1/2} \hat{f}_t$ converges to a four times continuously differentiable Gaussian process. The Karhunen–Loève (KL) expansion of Brownian motion is used to develop the limit theory in this case. Theorem 3.1 and Remark 3.2 provide the general finding for a fractional process with fractional Brownian motion limit with Hurst parameter $H \in (0,1)$ that embeds the Brownian motion case. In particular for $H = \frac{1}{2}$, we get the specialization*

$$G_\infty^{\frac{1}{2}} = \sum_{k=1}^{\infty} \frac{1}{\mu((k-\frac{1}{2})\pi)^4 + 1} \frac{\sin(k-\frac{1}{2})\pi r}{(k-\frac{1}{2})\pi} U_k' + \sum_{k=1}^{\infty} \left(\frac{1}{k\pi} - \frac{1}{\mu(k\pi)^4 + 1} \frac{\cos k\pi r}{k\pi} \right) V_k', \tag{30}$$

where $U'_k \sim N(0,1)$ and $V'_k \sim N(0,1)$. While the expression (30) differs from that given in PJ(2021, Theorem 3), the limit process is the same. Further, when $\mu = 0$ we have

$$G_\infty^{\frac{1}{2}}|_{\mu=0} = \sum_{k=1}^\infty \frac{\sin(k-\frac{1}{2})\pi r}{(k-\frac{1}{2})\pi}U'_k + \sum_{k=1}^\infty \frac{1-\cos k\pi r}{k\pi}V'_k = B(r), \tag{31}$$

as given in (15).

Remarks 3.7. *The sample paths of fBM are nowhere differentiable just like Brownian motion. But as the Hurst parameter H increases, these paths become smoother as indicated by their Hölder continuity property of order stictly less than H. It follows that for larger values of $H > 1/2$, the HP filter may reasonably be expected to perform better in trend determination because it seeks to capture a smoother process than Brownian motion. Simulations reported in Figure 1 of Section show that such improvements do occur as H increases.*

4 Asymptotic Theory of the Boosted Hodrick-Prescott Filter

From Theorem 3.1 and the following discussion it is evident that use of the HP filter does not lead to consistent estimation of a fractional Brownian motion stochastic trend when the tuning parameter $\lambda = O(n^4)$. In such cases, the HP estimated cycle inherits some of the trend characteristics in the underlying long memory time series. PS (2021) showed how this shortcoming can be remedied in the Brownian motion case by repeated application of a boosting algorithm.

The boosting procedure involves iteration of the HP filter m times on successive HP fitted residuals. Let the estimated fitted trend from the HP filter be $\hat{f} = S_n^\lambda x$ with $S_n^\lambda = (I_n + \lambda D_2 D'_2)^{-1}$, which employs the same twice-differencing matrix operator D'_2 used in (17), and $\hat{c} = (I_n - S_n^\lambda)x$. As the mechanism of bHP filter suggests, we apply the HP filter on $\hat{c}$. So the new estimate of the error is $\hat{c}^{(2)} = (I_n - S_n^\lambda)\hat{c} = (I_n - S_n^\lambda)^2 x$. Thus m iterations of the HP filter lead to the revised cyclical and trend estimates

$$\hat{c}^{(m)} = (I_n - S_n^\lambda)^m x \tag{32}$$

$$\hat{f}_t^m = x - \hat{c}^{(m)} = B_m^\lambda x, \tag{33}$$

where $B_m^\lambda = I_n - (I_n - S_n^\lambda)^m$, I_n is the $n \times n$ identity matrix. PS (2021) named this iterated process the boosted HP (bHP) filter in view of its similarity to L_2-boosting in regression applications.

As discussed in PS (2021), the HP filter can be thought of as a 'weak base learner' in the language of machine learning. The intuition behind the procedure is that the basic HP filter, when it is applied once with a given dataset, is too weak to learn enough from the data to capture the underlying trend in the time series. But when it is applied multiple times on the same data, boosting improves the method's learning capability at each iteration. In this way, the bHP filter provides the opportunity for improved trend capture over the HP filter applied to a given set of data with a conventional choice of the tuning parameter λ such as that commonly used in applied macroeconomics with the setting $\lambda = 1600$ for quarterly data.

Following the same approach as PS (2021), we develop a limit theory that shows how the bHP filter asymptotically enhances the performance of the HP filter when applied to fractionally integrated data precisely in those circumstances where the HP filter is itself inconsistent. Two

cases are considered dealing with fractional stochastic trends with and without accompanying drift mechanisms. The first result considers the case without drift.

Theorem 4.1. *Suppose x_t satisfies the functional law* (22) *and assume that the probability space is expanded so that $\frac{x_{\lfloor nr \rfloor}}{n^H} \to B_H(r)$ a.s.. Suppose further that the HP filter is iterated m times based on the bHP algorithm with $\lambda = \mu n^4$ and μ fixed. If $\mathrm{m} \to \infty$ as $n \to \infty$, then*

$$\frac{\hat{f}^{\mathrm{m}}_{\lfloor nr \rfloor}}{n^H} \xrightarrow{a.s.} B_H(r) = \sum_{k=1}^{\infty} \frac{\sin u_k r}{u_k} U_k + \sum_{k=1}^{\infty} \frac{1 - \cos v_k r}{v_k} V_k, \tag{34}$$

for $r \in (0,1)$ and $H \in (0,1)$. Further, if $\frac{1}{K_n} + \frac{K_n}{n} + \frac{K_n^4}{\mathrm{m}} \to 0$ as $n, \mathrm{m} \to \infty$,

$$\left| \frac{\hat{f}^{\mathrm{m}}_{\lfloor nr \rfloor}}{n^H} - \left(\sum_{k=1}^{K_n} \frac{\sin u_k r}{u_k} U_k + \sum_{k=1}^{K_n} \frac{1 - \cos v_k r}{v_k} V_k \right) \right| \longrightarrow 0 \ \ a.s., \tag{35}$$

for $r \in (0,1)$ and $H \in (0,1)$.

Remarks 4.2. *PS (2021, Theorem 1) showed that, in the case where $H = 1/2$ and the limit process is Brownian motion, the bHP filter is consistent under the same rate conditions. Theorem 4.1 extends their result to the general fractional case with $H \in (0,1)$. In particular, the estimated trend obtained from the bHP filter is consistent when the same tuning parameter setting $\lambda = \mu n^4$ is used as in the HP filter for which the trend estimate is inconsistent. Further, whereas the estimated trend produced by HP filter depends on the value of μ asymptotically, the estimated trend obtained from the bHP filter is asymptotically independent of the scale parameter μ.*

Remarks 4.3. *When $\mathrm{m} = 1$ the bHP filter is identical to the HP filter. As the number of iterations m increases, the bHP filter captures more fine grain details in the fractional process trend path. Correspondingly, when the underlying time series trend has an irregular path, as in the fractional process case, the bHP filter estimate becomes less smooth as m rises. The features of the bHP filter trend estimate are determined by both parameters λ and m but in such a way that increasing m for given λ enables the bHP filter to compensate for shortcomings in the base learner when $m = 1$. These features of the bHP filter are demonstrated in simulations reported in the next Section.*

In practical work it is common for economic and financial data to manifest both stochastic and deterministic trend properties. Deterministic drift functions can be a smooth or piecewise smooth functions interrupted by structural breaks. To accommodate such functions, we consider data generated by the superposition of a fractional process x_t with drift as

$$y_t = g_n(t) + x_t, \tag{36}$$

where $g_n(t)$ is a piecewise smooth interpolating function for which $\frac{g_n(\lfloor nr \rfloor)}{n^H} \to g(r)$ and x_t follows the functional law (22). We consider first the case where $g(\cdot)$ is a smooth deterministic function represented by a finite order trigonometric or time polynomial and establish consistent estimation of such trends by the bHP filter. We next consider more general continuous deterministic functions and piecewise continuous functions. The results follow closely from earlier analysis PJ & PS (2021; 2021) and are presented here as propositions.

Proposition 4.4. *Suppose the time series y_t is generated by* (36) *and $g(r)$ takes the form*

$$g(r) = \alpha_o + \sum_{k=1}^{M} \alpha_k \sin(2\pi kr) + \sum_{k=1}^{M} \beta_k \cos(2\pi kr), \tag{37}$$

where at least some α_k or $\beta_k \neq 0$ and $\max_k\{\alpha_k, \beta_k\} < \infty$. Then, in a suitably extended probability space

$$\frac{y_{\lfloor nr \rfloor}}{n^H} \to g(r) + B_H(r) \text{ a.s.,}$$

and

$$\left| \frac{\hat{f}^{\mathrm{m}}_{\lfloor nr \rfloor}}{n^H} - g(r) - B_H^{K_n}(r) \right| \to 0 \text{ a.s.,}$$

provided $\frac{K_n}{n} + \frac{K_n^4}{\mathrm{m}} \to 0$ as $n, \mathrm{m}, K_n \to \infty$, where $B_H^{K_n}(r) := \sum_{k=1}^{K_n} \frac{\sin u_k r}{u_k} U_k + \sum_{k=1}^{K_n} \frac{1-\cos v_k r}{v_k} V_k$ is a finite series approximation of $B_H(r)$.

In (37) M is considered fixed. If the function $g(r)$ has an infinite series representation with $M = \infty$ then a suitable summability condition must be imposed on the coefficients in (37) so that the trigonometric series converges uniformly.

Proposition 4.5. *Let y_t follow* (36) *and suppose $g(r)$ takes the time polynomial form*

$$g(r) = \beta_k r^k + \beta_{k-1} r^{k-1} + \cdots + \beta_0 \ \text{ where } \beta_i \neq 0 \text{ for some } i \leq k.$$

Then

$$\frac{y_{\lfloor nr \rfloor}}{n^H} \to g(r) + B_H(r) \text{ a.s.}$$

and

$$\left| \frac{\hat{f}^{\mathrm{m}}_{\lfloor nr \rfloor}}{n^H} - g(r) - B_H^{K_n}(r) \right| \to 0 \text{ a.s.,}$$

as $n \to \infty$ and $\mathrm{m} \to \infty$.

The HP filter is known (PJ, 2021) to preserve a polynomial drift up to degree 3 when $n \to \infty$. The bHP filter extends this capability as $m \to \infty$ to replicate polynomials of higher degree (PS, 2021). Propositions 4.4 and 4.5 show that comparable results are achieved in the presence of a fractional stochastic trend x_t by using the bHP filter. These propositions can be further extended to allow for a drift function $g_n(t)$ such that $\frac{g_n(\lfloor nr \rfloor)}{n^H} \to g(r)$ pointwise, where $g(r)$ is any continuous function or any piecewise continuous function, as considered in the following two results.

Theorem 4.6. *Suppose y_t follows* (36) *with $\frac{g_n(\lfloor nr \rfloor)}{n^H} \to g(r)$ pointwise and x_t satisfies the functional law* (22) *and $g(r)$ is a continuous function. Then the bHP filter when applied to y_t with $\lambda = \mu n^4$ has the following asymptotics*

$$\frac{y_{\lfloor nr \rfloor}}{n^H}, \frac{\hat{f}^{\mathrm{m}}_{\lfloor nr \rfloor}}{n^H} \to g(r) + B_H(r) \text{ a.s., } \text{ for } r \in (0,1) \tag{38}$$

as $n, \mathrm{m} \to \infty$.

In applications it can be useful to assume that the drift function $g(\cdot)$ has a finite number of structural break points or jump discontinuities. Acccordingly, suppose $g(\cdot)$ has b such points of jump discontinuity at $0 < r_1 < \cdots < r_b < 1$, leading to the following forms involving time and trigonometric polynomials

$$
g(r) = \begin{cases}
\alpha_{0,0} + \alpha_{0,1}r + \cdots + \alpha_{0,M_0}r^{M_0} & \text{if } r \in [0, r_1), \\
\vdots \\
\alpha_{l,0} + \alpha_{l,1}r + \cdots + \alpha_{l,M_l}r^{M_l} & \text{if } r \in [r_l, r_{l+1}), \\
\vdots \\
\alpha_{b,0} + \alpha_{b,1}r + \cdots + \alpha_{b,M_b}r^{M_b} & \text{if } r \in [r_b, 1],
\end{cases}
\tag{39}
$$

and

$$
g(r) = \begin{cases}
\alpha_{0,0} + \sum_{k=1}^{M_0} \alpha_{0,k}\sin(2\pi kr) + \sum_{k=1}^{M_0} \beta_{0,k}\cos(2\pi kr) & \text{if } r \in [0, r_1) \\
\vdots \\
\alpha_{l,0} + \sum_{k=1}^{M_l} \alpha_{l,k}\sin(2\pi kr) + \sum_{k=1}^{M_l} \beta_{l,k}\cos(2\pi kr) & \text{if } r \in [r_l, r_{l+1}), \\
\vdots \\
\alpha_{b,0} + \sum_{k=1}^{M_b} \alpha_{b,k}\sin(2\pi kr) + \sum_{k=1}^{M_b} \beta_{b,k}\cos(2\pi kr) & \text{if } r \in [r_b, 1]
\end{cases}
\tag{40}
$$

for some finite positive integers $M_0, \cdots, M_b$.

Proposition 4.7. *Suppose y_t follows (36) with $\frac{g_n(\lfloor nr \rfloor)}{n^H} \to g(r)$ pointwise and x_t follows the functional law (22). If $g(r)$ is any piecewise continuous function of the form (39) or (40), then as $\frac{1}{m} + \frac{m}{n} \to 0$,*

$$
\frac{\hat{f}^{\mathrm{m}}_{\lfloor nr \rfloor}}{n^H} \xrightarrow{a.s.} \begin{cases}
g(r) + B_H(r) & \text{if } r \in (0, 1) \setminus \{r_1, \cdots, r_b\} \\
\frac{1}{2}[g(r_i-) + g(r_i+)] + B_H(r) & \text{if } r = r_i \text{ for some } i \leq b,
\end{cases}
\tag{41}
$$

where $g(r_i-)$ and $g(r_i+)$ are the left and right limits of $g(r)$ at the break point r_i.

Theorem 4.8. *Suppose y_t follows (36) with $\frac{g_n(\lfloor nr \rfloor)}{n^H} \to g(r)$ pointwise for $r \in [0, 1]$ and x_t follows the functional law (22). If $g(r)$ is any piecewise bounded continuous function with breaks at $\{r_1, r_2, ..., r_b\}$, then as $\frac{1}{m} + \frac{m}{n} \to 0$,*

$$
\frac{\hat{f}^{\mathrm{m}}_{\lfloor nr \rfloor}}{n^H} \xrightarrow{a.s.} \begin{cases}
g(r) + B_H(r) & \text{if } r \in (0, 1) \setminus \{r_1, \cdots, r_b\} \\
\frac{1}{2}[g(r_i-) + g(r_i+)] + B_H(r) & \text{if } r = r_i \text{ for some } i \in \{1, 2, ..., b\},
\end{cases}
\tag{42}
$$

where $g(r_i-)$ and $g(r_i+)$ are the left and right limits of $g(r)$ at the break point r_i.

These results show consistency of the bHP filter under the stated conditions for trend functions composed of fractional processes and deterministic continuous drift functions. When the dift function has a finite number of structural breaks or jump discontinuities, the bHP filter is consistent everywhere except for the break points at which points the limit form of the bHP filter is given by the mid-point of the trend-break, analogous to a Fourier series representation of a piecewise continuously differentiable function.

5   Simulations, Implementation and Empirics

This section reports the results of simulation exercises and real data analyses to illustrate the effects of bHP filter estimation of stochastic trends involving nonstationary long memory time series. A stopping time for practical implementation of the boosting algorithm is provided following PS (2021), and its use is evaluated in simulations. Empirical applications to US interest rates and unemployment rate series are reported at the end of this section.

5.1   Simulations

Finite sample performance of the HP and bHP filters is examined for nonstationary trending time series with various values of the memory parameter d in the innovation process. We consider several data generating processes representative of empirical economic data and study the bHP filter's performance in terms of bias, variance, and mean squared error (MSE). The data-determined stopping rule criterion for the boosting iteration suggested in PS (2021) and the related automated version of the bHP filter are used in the simulations.

5.1.1   HP Filter for Different Values of d

According to Remark 3.7, the HP filter may reasonably be expected to perform better in trend determination for larger values of $H > 1/2$. Accordingly, we conduct a simulation exercise by incorporating ARFIMA in the data generating process. The simulation design is as follows. First, let $u_t^{(z)}$ be a stationary ARFIMA$(0, d^*, 0)$ time series as given by (2), $u_t^{(e)} \sim$ iid $\mathcal{N}(0, 1)$ be independent $u_t^{(z)}$, and $g_n(t)$ be a deterministic sequence. Define:

$$z_t = z_{t-1} + u_t^{(z)} \equiv I(d) \text{ with } 1 + d^* = d \in (0.5, 1.5) \text{and } d^* \in (-0.5, 0.5) \tag{43}$$
$$e_t = 0.5e_{t-1} + u_t^{(e)} + u_{t-1}^{(e)},$$
$$\tilde{x}_t = g_n(t) + z_t,$$
$$x_t = \tilde{x}_t + e_t. \tag{44}$$

In the specification (43) z_t is an $I(d)$ process generated as a random walk whose step size $u_t^{(z)}$ is an ARFIMA$(0, d^*, 0)$ time series. In (44) e_t is an ARMA$(1, 1)$ stationary process, $\tilde{x}_t$ is a trend process consisting of a non-random drift component $g_n(t)$ and the stochastic trend component z_t, and x_t is the observed time series, which allows for stationary deviations or measurement error in observations of $\tilde{x}_t$.

In this simulation the performance of the HP filter is assessed for different values of the memory parameter d. Based on (44), paths of x_t of length $n = 100$ are generated for each $d = \{0.55, 0.7, 0.85, 1.15, 1.3, 1.45\}$ (i.e., with $d^* = \{-0.45, -0.3, -0.15, 0.15, 0.3, 0.45\}$). For this first simulation $g_n(t) \equiv 0$ and $1,000$ replications are conducted. The HP filter is applied with $\lambda = 1600$ giving the filtered series $\hat{x}_t$ and a standardized sum of squared errors (StSSE) is computed:

$$StSSE = \frac{\sum_{t=1}^{100} (\tilde{x}_t - \hat{x}_t)^2}{\text{Var}(\tilde{x}_t)}.$$

Figure 1 shows histogram counts of StSSE for various values of d. These indicate that as d increases StSSE decreases. This finding is explained by the properties of the limit process. After appropriate standardization $\tilde{x}_t$ converges to a Type I fBM as in (3) with $H = d - 1/2$ for $d \in [1, 1.5]$. As H increases, the path of the Type I fBM becomes smoother by virtue of the Hölder condition. Increasing smoothness in the limiting trend process enables the HP filter, which is itself a smoother, to deliver improved estimates of the underlying trend. On the other hand, as d increases, the variability of $\tilde{x}_t$ increases. Hence, instead of working with a sum of squared errors (SSE) criterion, we use StSSE to compare the histograms. The plots reveal increased efficiency of the HP filter as d increases over the entire range $(0.5, 1.5)$. Analogous results (not reported here) were obtained with data generated from the same model but with z_t replaced by $\tilde{z}_t$ as in (11).
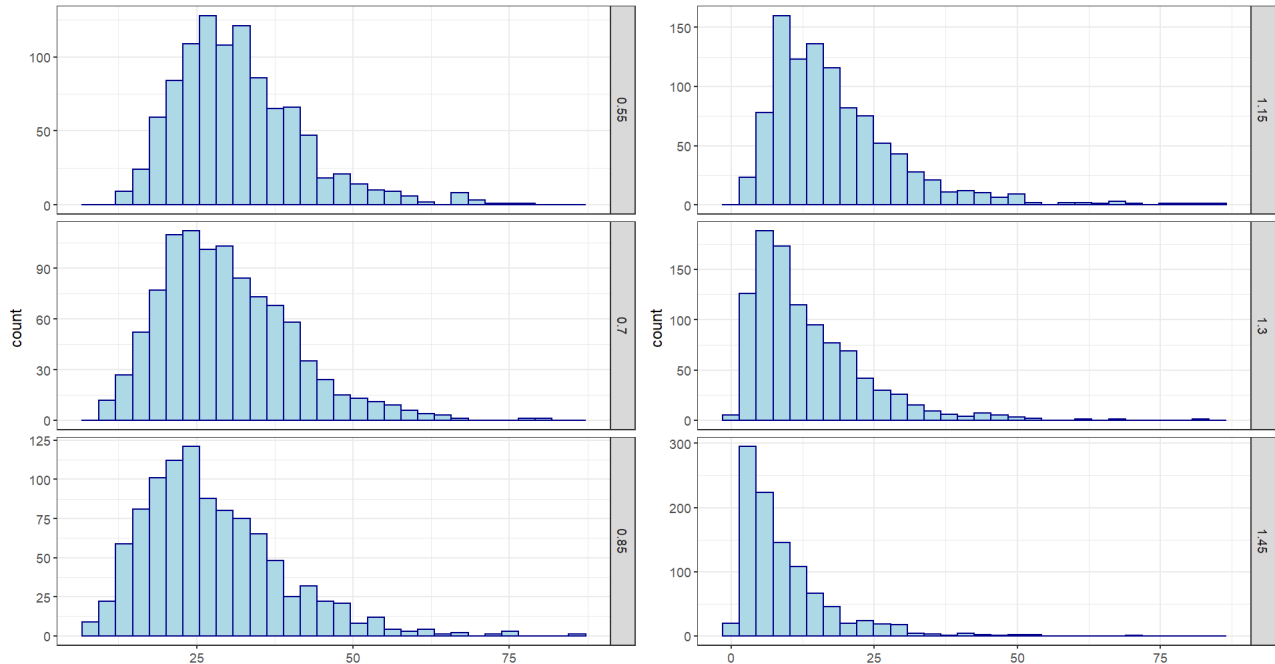

Figure 1: Histograms of the StSSE of the estimated trend by the HP filter with $\lambda = 1600$ based on a $1{,}000$ replications. The simulation is performed as described in (44) with $g_n \equiv 0$ and $d = 0.55, 0.7, 0.85, 1.15, 1.3, 1.45$.

5.1.2 Predicting Trend with Different Values of m

As shown in Theorem 3.1 the HP filter does not typically restore the underlying trend even asymptotically. Boosting the filter is computationally tractable and provides a more robust method of isolating the trend function in a nonstationary time series. As discussed in Remark 4.3, the boosted filter employs two tuning parameters, λ and m, in trend extraction, the choice of λ usually being given by that of the HP filter itself and the boosting iteration parameter m aiding identification of local as well as global trend behavior.

This simulation exercise explores how boosting can enhance HP filter performance and capture more long term features in the data as m increases. We consider three cases: a stochastic trend without any deterministic trend, a stochastic trend with a continuous drift, and a stochastic trend with a piecewise continuous function. Data of length $n = 100$ are generated as described in (44)

Type	Equation
Stochastic Process without Drift	$g_n(t) \equiv 0$
Stochastic Process with Continuous Drift	$g_n(t) = 10 \left(\frac{t}{n}\right)^2 + 30 \left(\frac{t}{n}\right)^4$
Trend-break Stochastic Process	$g_n(t) = 20 \mathbb{I}(t > 0.5n + 1)$

Table 1: The form of the deterministic trend

with error e_t replaced by $e_t^0 = -0.5e_{t-1}^0 + u_t^{(e)} + u_{t-1}^{(e)}$ and the structure of $g_n(t)$ used in the simulation is given in Table 1. We use $\lambda = 1600$ for this simulation, as in typical quarterly data economic applications.
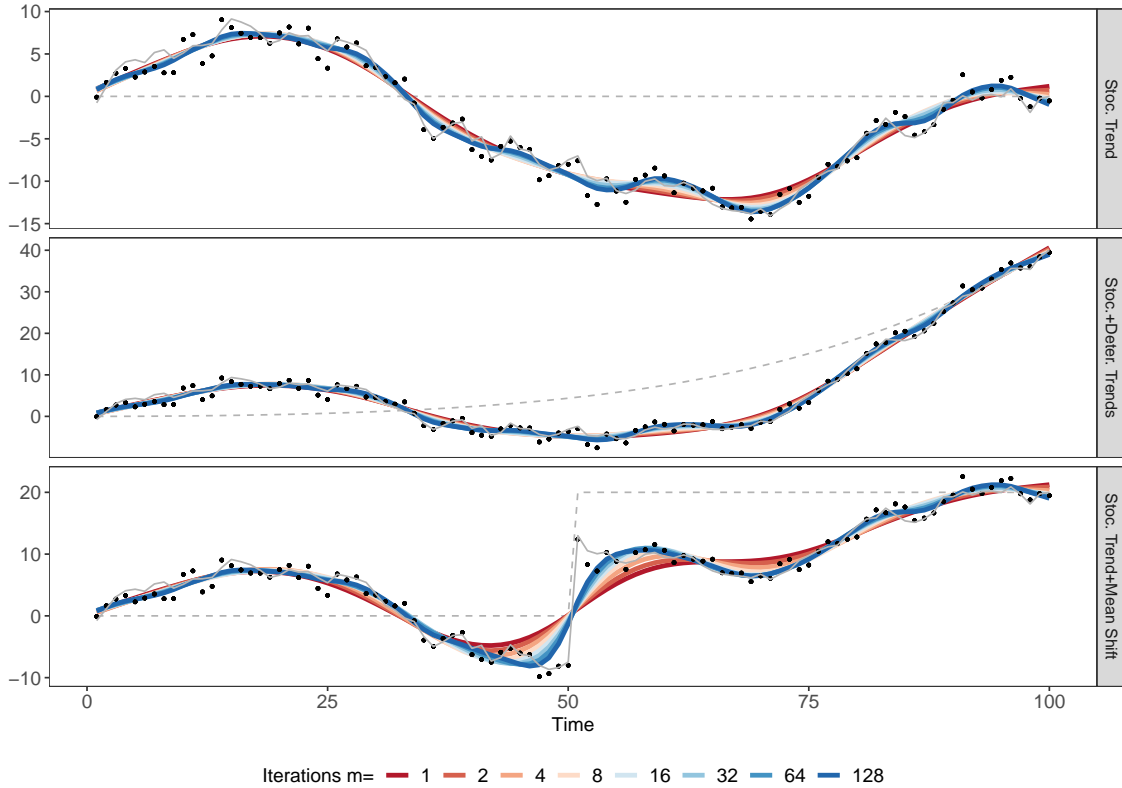

Figure 2: In each panel, observations x_t are shown by black dots, the underlying trend process $\tilde{x}_t$ by the solid gray lines, the deterministic trend $g_n(t)$ by the dashed gray lines, and the fitted trend lines obtained by the HP filter (red line) and bHP filters (lines colored sequentially from red to blue). The stochastic trend component z_t is an $I(1.25)$ time series for $\tilde{x}_t$ generated as in (44).

The results are presented in Figures 2 and 3 for $I(1.25)$ and $I(0.75)$ stochastic processes z_t, respectively. In each figure, black dots represent observations x_t, the solid gray line is the stochastic trend $\tilde{x}_t$ and the dashed gray line is the deterministic trend $g_n(t)$. According to Theorem 4.1, the estimated trend should improve as the HP filter is iterated. The red line gives the estimated trend obtained by the HP filter. The sequential lines from red to blue show how that estimate is refined and reflects more detail of the underlying trend for $\mathrm{m} = 2, 4, 8, 16, 32, 64, 128$. For the trend break process, the estimated trend by the bHP filter undergoes a smooth transition at the break

point $t = 50$. The transition is more rapid as the number of iterations increase and the value at the breakpoint is close to the average of the immediate values on both sides of the breakpoint, as asymptotic theory predicts. For the case $d = 0.75$, the pattern is similar to that of $d = 1.25$ as the HP filter is iterated from 1 to 128. Clearly, boosting works better than the HP filter in both cases. The figures also suggest that the estimate becomes stable after sufficiently large m and changes little with further iterations. The stability of the bHP filter is further investigated in Section 5.1.3. In sum, the bHP filter evidently captures a smoothed version of the underlying trend in the observed data. This conclusion is consistent with simulation results for the special unit root case $d = 1$ in PS (2021).
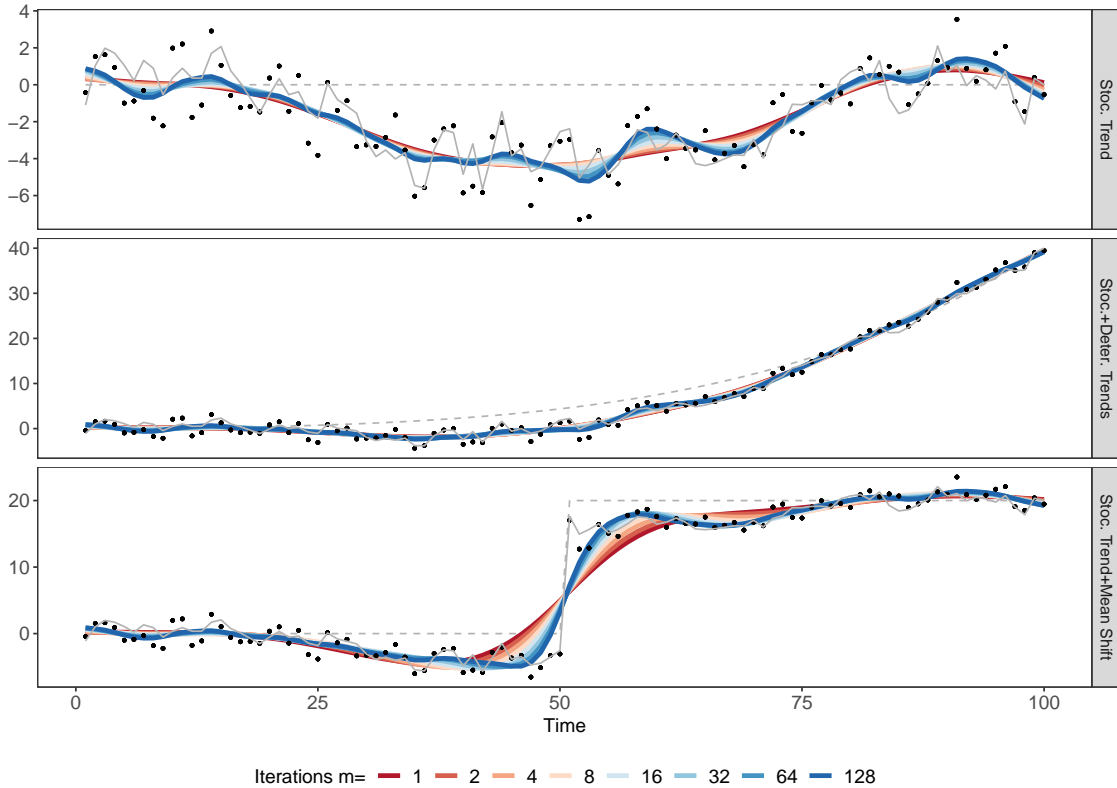

Figure 3: In each panel, observations x_t are shown in black dots, the underlying trend process $\tilde{x}_t$ by the solid gray lines, the deterministic trend $g_n(t)$ by the dashed gray lines, and the fitted trend lines obtained by the HP filter (red line) and bHP filters (lines sequentially colored from red to blue). For the stochastic trend component z_t, an $I(0.75)$ process is used to generate x_t in (44).

5.1.3 Bias-Variance Trade-Offs in Boosting

Bias reductions in statistical estimation often lead to a rise in variance. Similar effects occur with boosting as variance tends to increase with each iteration of the boosted filter. This section reports the findings of simulations that were conducted to explore how bias, variance, and MSE change with boosting iterations of the filter. For this analysis, the following five DGPs similar to those of PS (2021, Section 3) were employed.

- **DGP 1:** The data are generated as in (44) with $g_n(t) = 500(\frac{t}{n})^3$.

- **DGP 2:** DGP 1 but with $g_n(t) = 500(\frac{t}{n})^4$.

- **DGP 3:** DGP 1 but with $g_n(t) = 5t^{\frac{1}{5}}\cos(0.05\pi t^{0.09})$, a deterministic sinusoidal trend.

- **DGP 4:** DGP 1 but with $g_n(t) = \cos(0.5\pi t)$ to emulate a time-dependent periodic pattern often present in economic data, interpreted as a cycle.

- **DGP 5:** DGP 3 with the stochastic trend z_t replaced by

$$z_t^{(1)} = u_t^{(z)}\mathbb{I}(t < 0.5n) + \left(\frac{t - 0.5n}{n} - \sum_{j=\lfloor 0.5n \rfloor}^{t} u_t^{(z)} \right)\mathbb{I}(t \geq 0.5n),$$

giving a stationary first half trajectory followed by a partial sum process.

The simulation design for the computation of bias, variance and MSE is given in the following algorithm, with a sample size $n = 100$ unless otherwise indicated.

- **Step 1:** Simulate $\tilde{x}_t$ as a combination of stochastic and deterministic trends according to (44).

- **Step 2:** Generate measurement errors e_t and data using $x_t = \tilde{x}_t + e_t$, calculate the bHP filter from the data with $\lambda = 1600$ and iteration parameter m settings from 1 to 40. Repeat 50 times to find the bias variance and MSE of the bHP estimates of the trend process $\tilde{x}_t$.

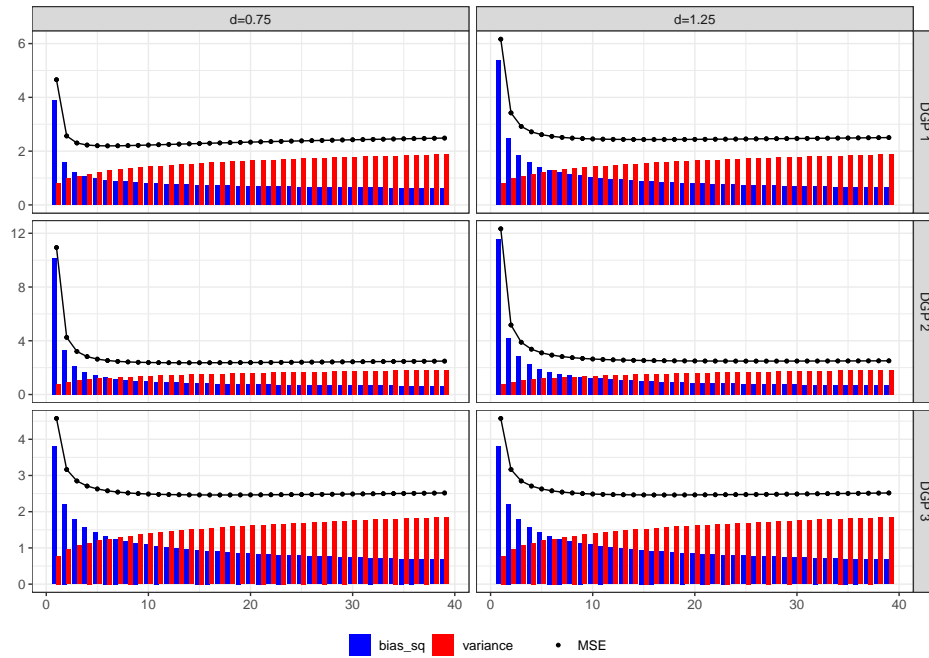- **Step 3:** Repeat 100 times to compute the average bias, variance, and MSE for each m.

Figure 4: The plots show the bias, variance and MSE of the estimated trend obtained by the bHP filter for DGPs 1-3 when $\lambda = 1600$ and $d = 0.75, 1.25$.

Figure 4 shows the bias, variance and MSE of the estimated bHP filter trend for DGPs 1-3 when $\lambda = 1600$ and $d = 0.75, 1.25$. Squared bias drops significantly with a single iteration from $\mathrm{m} = 1$ to $\mathrm{m} = 2$ as does the MSE. Variance initially increments at a slow rate compared with bias reductions but the MSE stabilizes after a few boosting iterations, a finding that matches PS (2021, Section 3.1).

5.2 Stopping Time Criteria

As noted above, boosting can significantly improve trend estimation with several iterations but after the MSE stabilizes boosting additional iterations can lead to overfitting. Use of a suitable stopping criterion is therefore recommended for practical implementation. PS (2021) described two data-based methods for selecting the iteration number m. One method uses the ADF unit root test with a 5% significance level at each iteration until the test shows stationarity. This procedure is called bHP-ADF. The second method uses the following information criterion to control overfitting the observations

$$IC(m) = \frac{\hat{c}^{(\mathrm{m})'}\hat{c}^{(\mathrm{m})}}{\hat{c}^{HP'}\hat{c}^{HP}} + \log(n)\frac{\mathrm{tr}(B_{\mathrm{m}}^{\lambda})}{\mathrm{tr}(I_n - S_n^{\lambda})} \tag{45}$$

The resulting procedure is called bHP-BIC. The first term of (45) calculates the ratio of the error sum of squares obtained by the bHP filter, $\hat{c}^{(\mathrm{m})'}\hat{c}^{(\mathrm{m})}$ with m iterations relative to the error sum of squares of the HP filter $\hat{c}^{HP'}\hat{c}^{HP}$. The quantity $\mathrm{tr}(B_{\mathrm{m}}^{\lambda})$ measures effective degrees of freedom after applying the bHP filter with parameters (λ, m) and $\mathrm{tr}(I_n - S_n^{\lambda})$ the effective degrees of freedom after the HP filter. The ratio of these degrees of freedom scaled by $\log(n)$ gives the penalty term to control overfitting. The measure $\mathrm{tr}(B_{\mathrm{m}}^{\lambda})$ has the following asymptotic form as $n \to \infty$:

$$\mathrm{tr}(B_{\mathrm{m}}^{\lambda}) = n - \sum_{k=1}^{n-2} \frac{(\lambda\gamma_k^2)^{\mathrm{m}}}{(1 + \lambda\gamma_k^2)^{\mathrm{m}}}(1 + o(1)), \quad \gamma_k^2 = 4\left(1 - \cos\frac{k\pi}{n-1}\right)^2,$$

which is shown in PS (2021) to increase as m increases whereas $\partial\mathrm{tr}(\mathrm{B}_{\mathrm{m}}^{\lambda})/\partial\mathrm{m}$ decreases as m increases. When $\lambda = O(n^{\delta})$ for some $\delta > 0$ and m is finite, $\mathrm{tr}(B_{\mathrm{m}}^{\lambda}) \to 2$ and $[\mathrm{tr}(I_n - S_n^{\lambda}) - (n - 2)] \to 0$ as $n \to \infty$, so the penalty term has order $2\log(n)/n \to 0$ as $n \to \infty$.

Simulations were performed to investigate the effects of changing m as n increases with variations in λ according to the sample size n. For each pair $\{(d, n) : d = 0.55, 1.15, 1.45; n = 64, 128, 256\}$, 500 sample paths were generated as in (44) with a continuous drift $g_n(t)$ trend as given in Table 1. The bHP-BIC filter was implemented for $\lambda \in \{100, 1600, 25600\}$, roughly matching $\lambda \propto n^4$, in each of the simulated trajectories. Figure 5 plots histograms of the 500 resulting values of m for each n. Evidently, the optimal value of m selected by BIC tends to increase with the sample size n and therefore matching increases in λ in this experiment, allowing more iterations of the filter.

On the other hand, for a fixed λ, if n increases $\mathrm{tr}(B_{\mathrm{m}}^{\lambda})$ increases for any m and $\mathrm{tr}(I_n - S_n^{\lambda})$ decreases. Hence the penalty term increases, contributing to early termination of the iterations. Simulations were performed to monitor how the empirical distribution of m behaves for fixed λ but different values of the sample size n and d. The same combinations of d and n as before were used with fixed $\lambda = 1600$. Figure 6 shows that as n increases, the optimal m decreases for each d. Thus, the optimal m for $n = 256$ is left shifted relative to those for larger values of n, and the optimal m

for $n = 64$ is most skewed to the right, confirming that the number of iterations typically reduces as n increases given a fixed λ.
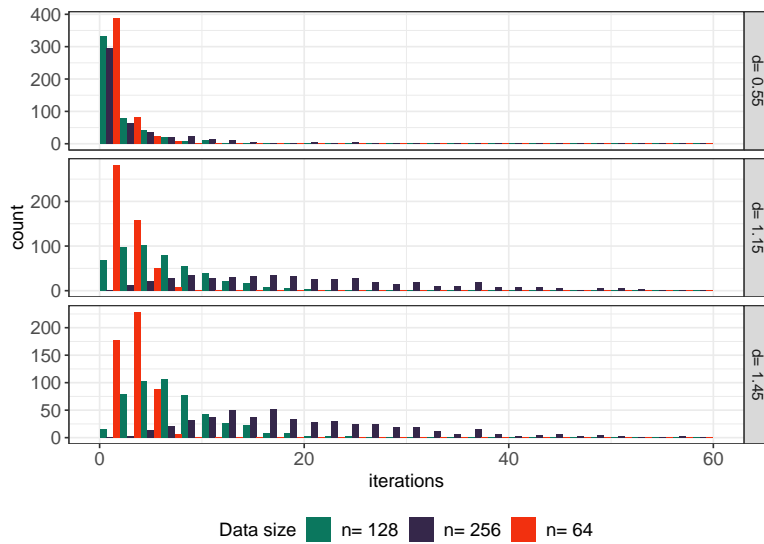

Figure 5: Stopping times for bHP-BIC with sample sizes $n \in \{64, 128, 256\}$, dependence parameter $d \in \{0.55, 1.15, 1.45\}$, $\lambda \in \{100, 1600, 25600\}$ varied according to n, and $g_n(t)$ generated as the continuous drift in Table 1.
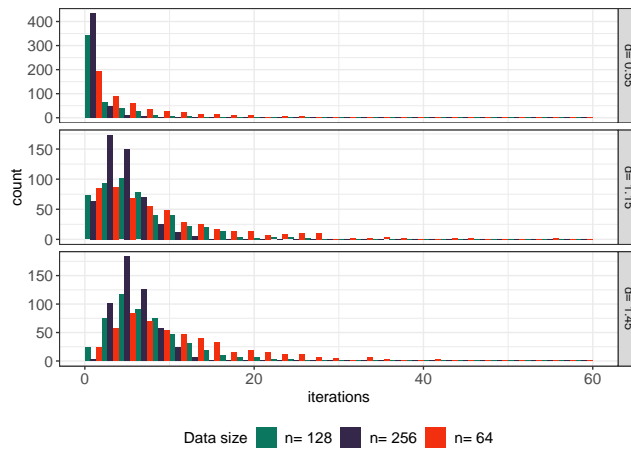

Figure 6: Stopping times for bHP-BIC with fixed $\lambda = 1600$, sample sizes $n \in \{64, 128, 256\}$, dependence parameters $d \in \{0.55, 1.15, 1.45\}$, and $g_n(t)$ the continuous drift in Table 1.

In the bias, variance, and MSE computations of Section 5.1.3, the values of m selected under bHP-ADF and bHP-BIC were also calculated. The results are shown in the histograms of Figure 7, which display 100 values of the average m obtained for DGPs 1-3 and for $d \in \{0.75, 1.25\}$ in the simulations. In the upper panel (DGP 1), where $g_n(t)$ is a cubic polynomial, about 20% of the average m obtained by bHP-ADF are less than 2; in the middle panel (DGP 2), where $g_n(t)$ is a 4th degree polynomial, fewer than 5% of the average m are below 2 . As indicated in PS (2021),

the HP filter does not remove higher-order polynomial trends without boosting and this property is evident in Figure 7 for both values of d. In the lower panel (DGP 3) more than 80% of the average number of iterations are less than 2.

Figure 7 shows that BIC selection produces many more iterations to minimize the information criterion, leading to histograms for m that are more scattered than those of the ADF selection for each of the DGPs and each value of d. The optimal m from BIC is also more scattered in the lower panel for DGP 3, which corresponds to the finding in Figure 4 that average bias and MSE decline more slowly for this DGP.
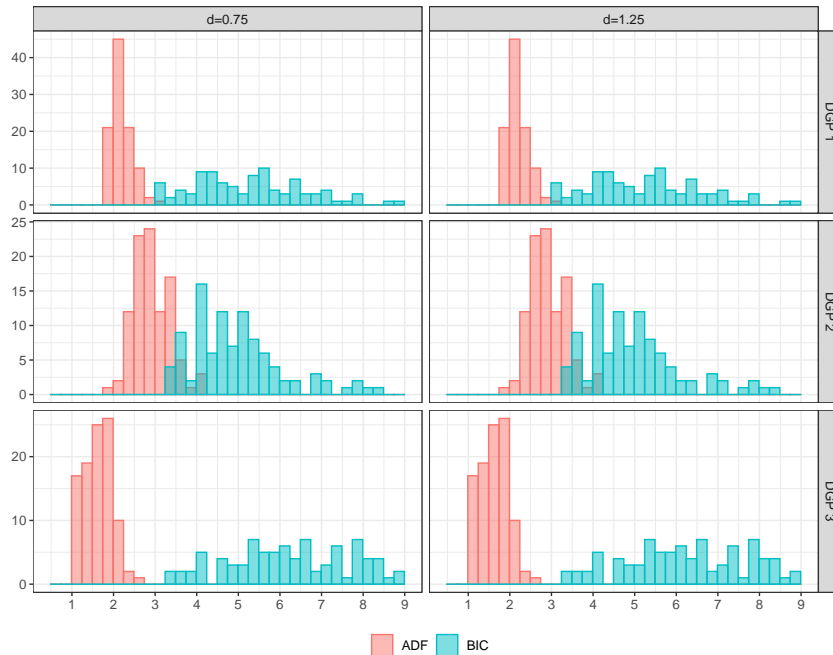

Figure 7: The distribution of the average number of iterations of the bHP filter with $\lambda = 1600$ shown for DGPs 1, 2, and 3 and for $d \in \{0.75, 1.25\}$.

	d	HP	bHP-ADF	bHP-BIC	AR(4)
Stoc. Trend	0.75	1.525147	1.338978	1.298727	3.248710
Stoc.+Deter. Trends	0.75	1.593383	1.383501	1.289304	3.697556
Stoc. Trend+Mean Shift	0.75	8.153291	6.075353	4.385433	8.568215
Stoc. Trend	1.25	3.912214	2.126089	1.352408	4.622455
Stoc.+Deter. Trends	1.25	3.964066	2.162909	1.368690	4.584532
Stoc. Trend+Mean Shift	1.25	9.529270	7.356215	3.927817	9.009112

Table 2: The MSE of the estimated trend computed using the HP, bHP-ADF, and bHP-BIC filters with $\lambda = 1600$ and an AR(4) model. The values $d \in \{0.75, 1.25\}$ were used in simulating the stochastic trend. The data are generated as in (44) and Table 1.

The HP and bHP filters were next compared with an AR(4) regression, a method frequently used in empirical work with quarterly economic data and recently recommended by Hamilton (2018).

Data were generated as in (44) and Table 1 with sample size $n = 100$. The HP, bHP-ADF, and bHP-BIC filters were computed, AR(4) models were fitted, and MSEs calculated ignoring the initial and end four points to enable comparisons with the AR(4) model as in PS (2021). Table 2 reports the results, which show that the AR(4) model produces the highest MSEs in fitting each of the trend processes and for each $d \in \{0.75, 1.25\}$. The AR(4) MSEs are almost three times those of the bHP-BIC filter. Both the HP filter and the bHP-ADF performed poorly for trajectories with a stochastic trend and mean-shift compared to bHP-BIC. For all scenarios, the bHP-BIC filter consistently outperformed the other approaches in trend determination.

Simulations were also conducted using the same model design (44) but an aggregation process for the stochastic trend defined by (11) which converges to a type II fBM upon suitable standardization, in place of the mechanism (43). The findings closely matched those given in Table 2 and are not reported here.

5.2.1   MSE for Different Values of λ and Comparison with AR(4) Model

This section provides histogram plots to assess the robustness of the bHP filter by monitoring the variation of its MSE according to different choices of λ. Data generation for this simulation is similar to that of 5.1.3. All combinations of DGP 3 and DGP4, $\lambda \in \{400, 800, 1200, 1600\}$, and $d \in \{0.75, 1, 1.25\}$ are employed. The algorithm is as follows.

- **Step 1:** Fix the value of d and the DGP. Simulate $\tilde{x}_t$ for the specific DGP and value of d.

- **Step 2:** Generate the error e_t of length 100 and the bHP-BIC is applied for different value of $\lambda = 400, 800, 1200, 1600$. This is repeated 50 times. The MSE and the average number of iterations are recorded.

- **Step 3:** Repeat the whole process 100 times to get 100 values for MSE and the average iterations.
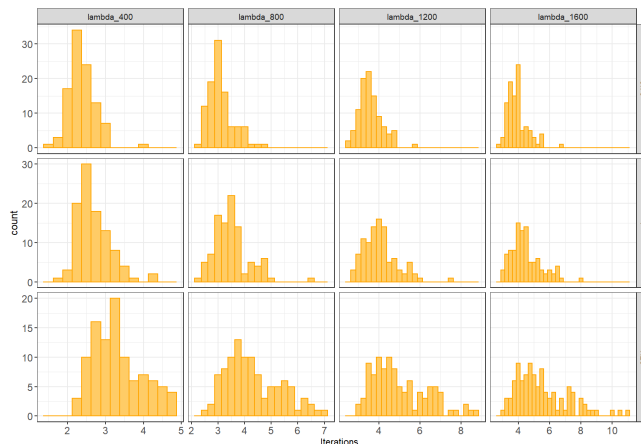

Figure 8: Distributions of the average number of iterations in the bHP-BIC filter for $\lambda \in \{400, 800, 1200, 1600\}$ and $d \in \{0.75, 1, 1.25\}$ using DGP 3.

Figures 8 and 9 show histograms of the number of iterations in filtering DGP 3 and DGP 4 with bHP-BIC. The number of iterations m increases as λ increases. As Remark 3.5 suggests, the

performance of the HP filter generally improves with smaller λ because the lower the penalty in (16) the greater the capacity of the filter to capture granularity or local behavior in a trajectory. Accordingly, it is expected that the boosted filter will need fewer iterations with smaller λ.
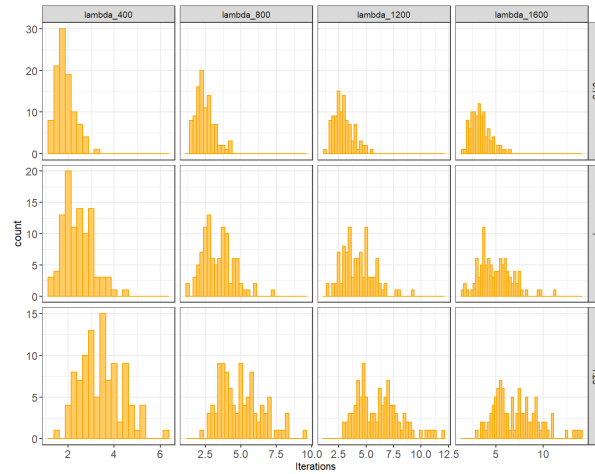

Figure 9: Distributions of the average number of iterations by the bHP-BIC filter for $\lambda \in \{400, 800, 1200, 1600\}$ and $d \in \{0.75, 1, 1.25\}$ using DGP 4.
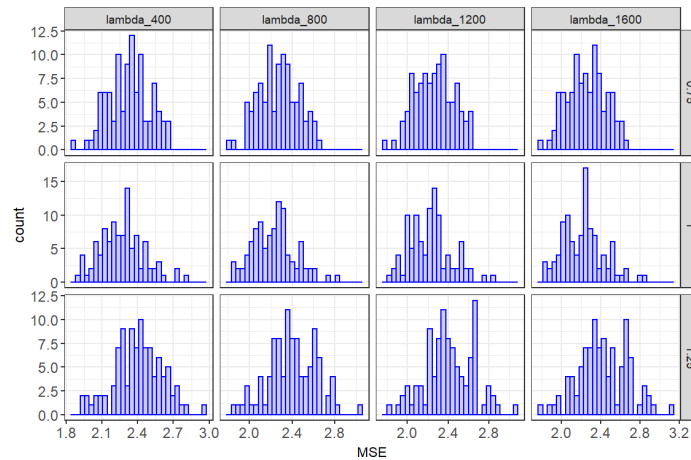

Figure 10: Distribution of the average MSE of the estimated trend from the bHP-BIC filter for $\lambda \in \{400, 800, 1200, 1600\}$ and $d \in \{0.75, 1, 1.25\}$ using DGP 3.
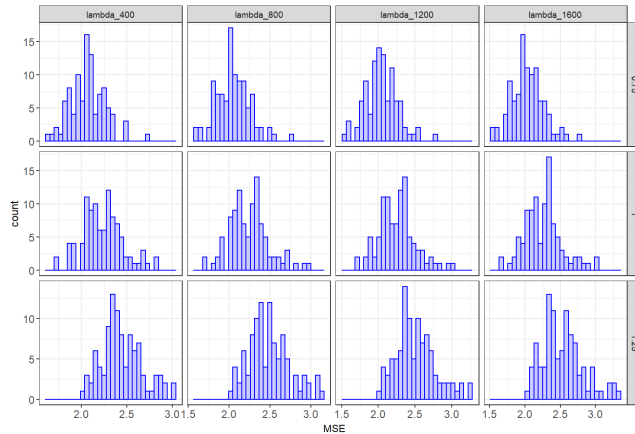
Figure 11: Distributions of the average MSE of the estimated trend by the bHP-BIC filter for $\lambda \in \{400, 800, 1200, 1600\}$ and $d \in \{0.75, 1.00, 1.25\}$ using DGP 4.

The next exercise aims to assess the performance of the HP, bHP-ADF, and bHP-BIC filters compared to that of an AR(4) regression. DGPs 1-5 are used to generate 200 samples. All five models are fitted and the MSEs calculated. To accommodate the AR(4) regression in the comparison, four initial and final points are eliminated. For DGPs 1-5, the values of d considered here are 0.75 and 1.25. For DGP 4, $g_n(t)$ is a periodic function with values between $[-1, 1]$ with periodicity 4, small enough in comparison to n so that $g_n(t)$ can be considered a cycle. The MSE under different DGPs are provided in Table 3.

	d	HP	bHP-ADF	bHP-BIC	AR(4)
DGP1	0.75	2.740997	2.696103	2.169544	6.165538
	1.25	4.108391	2.603417	2.486829	6.245990
DGP 2	0.75	4.684468	2.672197	2.407895	6.244237
	1.25	6.265164	2.603666	2.756768	6.261346
DGP 3	0.75	2.748083	2.698715	2.057356	5.817983
	1.25	4.423393	2.563303	2.473243	5.778962
DGP 4	0.75	1.811997	2.605251	1.930835	3.811153
	1.25	3.293247	2.534033	2.433160	5.293758
DGP 5	0.75	2.824658	2.823368	2.111107	6.178783
	1.25	3.430196	2.732810	2.271670	6.086447

Table 3: The MSE of the estimated trend computed using the HP, bHP-ADF, bHP-BIC and AR(4) uder different DGPs.

The MSEs of bHP-BIC and bHP-ADF are very similar in all cases and are less than the MSEs produced by the HP filter and the AR(4) regression. The underlying trends in DGPs 1 and 2 have time polynomials of order 3 and 4. For DPG 2, the HP filter has the highest MSE, as it fails to capture the 4th degree polynomial trend. DGP 3 reflects a slow-moving cycle with varying

magnitude depending on time. DGP 4 involves a small deterministic cycle of periodicity 4, and DGP 5 involves a break in the stochastic trend and the same cycle as DGP 3. In this variety of complex trend and cycle generating processes, the bHP filter successfully captures the underlying mechanism of each trend process and maintains a systematically low MSE throughout. The MSE of bHP-BIC is uniformly lower than that of bHP-ADF and is higher for $d = 1.25$ than $d = 0.75$.

5.3 Empirical Examples

This section reports empirical applications of the methodology to two examples where long memory is present in the data. Monthly data was collected for the U.S. effective federal funds rate (EFFR) and quarterly data were collected for the seasonally adjusted U.S. unemployment rate for the period 1973-2021[6]. Over these five decades seven U.S. recessions have been recorded by the NBER.[7] Considerable variation and a longer term drift are evident in the federal Funds rate with rates approaching 20% during the 1981 recession and rates falling to near zero following the GFC and again during the Covid 19 pandemic. The unemployment rate also fluctuates with high levels of unemployment following the 1981 recession, the GFC and during the covid 19 pandemic of 2020. The data are shown in Figure 12.
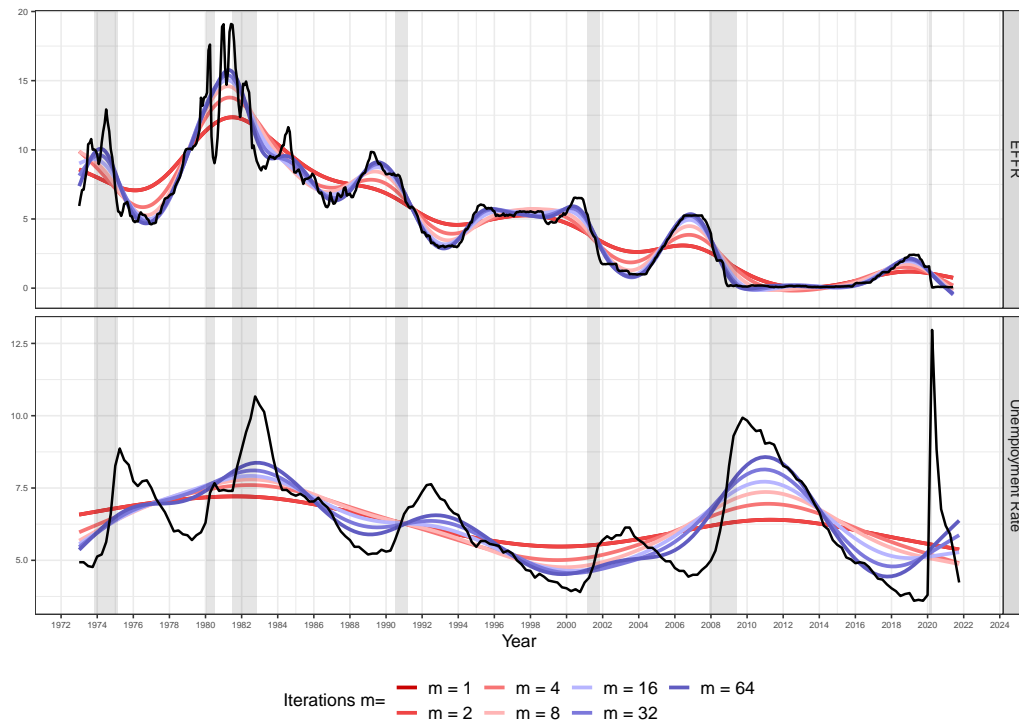

Figure 12: Estimated trends of the effective monthly Federal Funds rate and quarterly U.S. unemployment rates over 1973 2021 obtained from the bHP filter. Observations are shown by the solid black line and the bHP filter by colored lines for different values of m. Shaded areas are the NBER recorded U.S. recessions.

---

[6]The data are sourced from the St. Louis Fed (https://fred.stlouisfed.org.)

[7]See https://www.nber.org/research/business-cycle-dating.

For each of the time series the memory parameter d is estimated using the exact local Whittle procedure (Shimotsu and Phillips, 2005), which allows for both stationary and nonstationary long memory and enables valid confidence interval construction. The estimated values and confidence intervals are given in Table 4. Both the series show clear evidence of nonstationary long memory based on these estimates and confidence intervals. The underlying trend in the series is estimated using the HP and bHP-BIC filters. Since the unemployment rate data is collected quarterly and the EFFR series is monthly, the penalty parameters were set to $\lambda = 1600$ and $3^4 \times 1600$, respectively. AR(4) regressions were also fitted to the series to compare results from this method with the estimated trend behavior obtained from the HP and automated bHP filters.

Data set	Bandwidth Parameter	Value of d	Confidence Interval
Monthly EFFR	$582^{0.7}$	0.879	(0.7736, 0.9838)
Quarterly Uemployment Rate	$196^{0.7}$	0.842	(0.6886, 0.9947)

Table 4: Confidence intervals for d obtained from exact local Whittle estimation.

Figure 12 shows how, with a rising number of iterations, the boosted HP filter captures more specific features of the data path and does so more prominently with the EFFR data while still smoothing over short run fluctuations and noise. However, as already discussed, after a certain number of iterations the HP filter changes the estimate negligibly with further iterations and can lead to overfitting. An automated bHP filter is therefore applied to avoid overfitting. The bHP-BIC used 26 iterations for the EFFR data and 99 iterations for the unemployment rate data in fitting the trends. The results are displayed in Figure 13 for the period 1973-2021. An AR(4) regression was also used and gave results that closely match the raw data, seemingly overfitting and failing to distinguish underlying trend behavior in the data. With autoregressive fitting the estimates are predictive and driven by immediately preceding values, whereas the bHP filter uses data from the past and future to estimate trend behavior and direction at each time point, except for a few terminal points in the data. In consequence, AR fitting is highly impacted by local behavior in the data and susceptible to short run noise contamination of the underlying trend.

Figure 14 provides a snapshot of how the HP, bHP-BIC, and the AR(4) methods perform over January 1990 to December 2010. During this period, there are multiple peaks and valleys along the paths of both time series with three recession periods. The HP filter notably underperforms in revealing the magnitude of the rate hikes and drops over these periods and by failing to capture the transitions. On the other hand, the autoregression estimates suffer from markedly overfitting the data. Use of boosting enables the bHP-BIC filter to capture more of the trend paths and directions in the data than the HP filter, while resisting the evident overfitting of autoregressive methods. These findings corroborate other recent empirical evidence concerning the use of autoregressions, HP filtering and boosted filtering in business cycle research (Hall and Thomson, 2021, 2022; Mei et al., 2022).
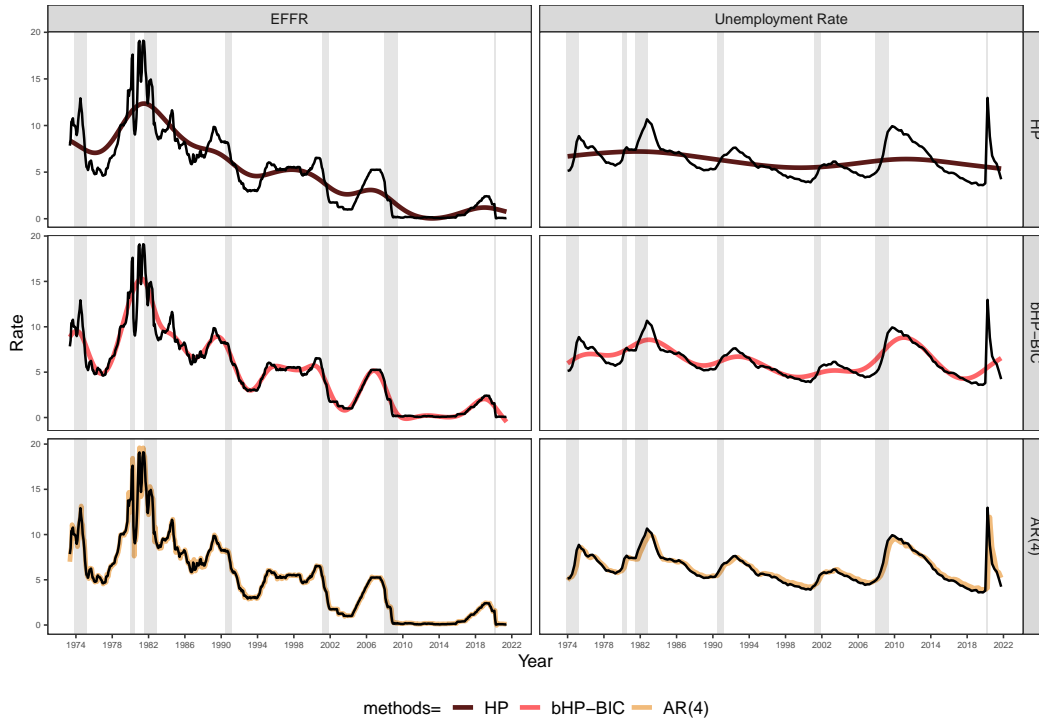
Figure 13: Estimated trends of effective monthly Federal Funds rates and quarterly U.S. unemployment rates from 1973- 2021 obtained by HP, bHP-BIC and AR4 regression methods. The actual data are shown by the black lines. The shaded regions show the NBER recorded recessions.
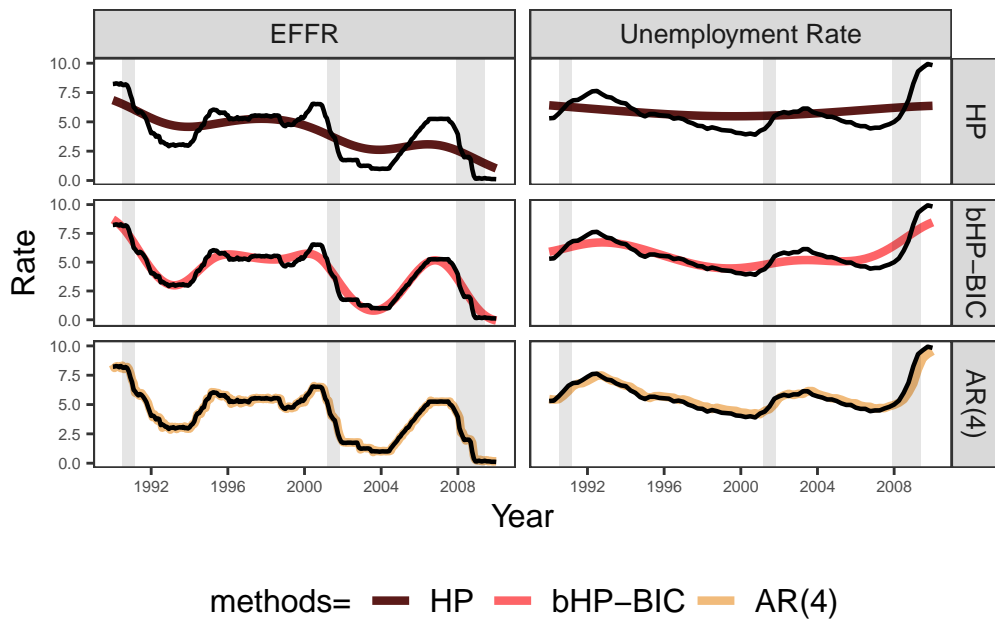

Figure 14: Estimated trends in effective monthly Federal Funds rates and quarterly U.S. unemployment rates from January 1990- December 2010 obtained by the HP, bHP-BIC and AR(4) regression methods. The shaded regions show the NBER recorded recessions.

6 Conclusion

This paper develops asymptotic theory for smoothing filters that are used to estimate the underlying trends in time series data, with a focus on the properties of the Hodrick-Prescott filter and its recently developed boosted version allowing for a wide class of nonstationary time series with possibly fractional stochastic process limits. Earlier research had shown that in the case of time series with a unit root where the normalized series converges to Brownian motion the HP filter fails to remove the stochastic trend even asymptotically. To mitigate this weakness, recent research suggested boosting the HP filter by iterating the filter and established that this procedure delivers a consistent estimate of the trend and improves finite sample performance of both the fitted trends and residual cycle elements in cases of unit root and deterministic trending time series. The current paper extends these results to a much wider class of nonstationary long range dependent time series with fractional stochastic process limits. The analysis reveals that the HP filter produces inconsistent trend and cycle estimates within this wider class and that boosting enables consistent estimation. The same benefits of boosting continue to hold for time series with deterministic drifts and possible structural breaks.

7 Appendix A: Proofs

Proof of Theorem 3.1:

i. To prove part (i), we rely on the following two preliminary steps. Step 1 proves weak convergence of the finite dimensional distributions of $\{G_l^H(r) : r \in [0, 1]\}$ to the finite dimensional distributions of $\{G_\infty^H(r) : r \in [0, 1]\}$. Step 2 shows that the sequence $G_l^H(\cdot)$ is asymptotically tight in $C[0, 1]$.

Step 1: G_l^H is a Gaussian process with zero mean and covariance function

$$
\begin{aligned}
\mathrm{Cov}(G_l^H(r), G_l^H(s)) = & \sum_{k=1}^{l} \frac{(\sin u_k r)(\sin u_k s)}{(\mu u_k^4 + 1)^2 u_k^2} \mathrm{Var}(U_k) \\
& + \sum_{k=1}^{l} \left[\frac{1}{v_k} - \frac{1}{\mu v_k^4 + 1} \frac{\cos v_k r}{v_k} \right] \left[\frac{1}{v_k} - \frac{1}{\mu v_k^4 + 1} \frac{\cos v_k s}{v_k} \right] \mathrm{Var}(V_k) \\
:= & I_{01}^l + I_{02}^l.
\end{aligned}
$$

G_∞^H is a Gaussian process with zero mean and covariance function

$$
\begin{aligned}
\mathrm{Cov}(G_\infty^H(r), G_\infty^H(s)) = & \sum_{k=1}^{\infty} \frac{(\sin u_k r)(\sin u_k s)}{(\mu u_k^4 + 1)^2 u_k^2} \mathrm{Var}(U_k) \\
& + \sum_{k=1}^{\infty} \left[\frac{1}{v_k} - \frac{1}{\mu v_k^4 + 1} \frac{\cos v_k r}{v_k} \right] \left[\frac{1}{v_k} - \frac{1}{\mu v_k^4 + 1} \frac{\cos v_k s}{v_k} \right] \mathrm{Var}(V_k) \\
:= & I_{01} + I_{02}
\end{aligned}
$$

Note that $\left|\sum_{k=1}^l \frac{(\sin u_k r)(\sin u_k s)}{(\mu u_k^4+1)^2 u_k^2}\mathrm{Var}(U_k)\right| < K_0 \left|\sum_{k=1}^\infty \frac{1}{u_k^2}\mathrm{Var}(U_k)\right|$ for some constant K_0 as $u_k = O(k)$. Now, $\mathrm{Var}(U_k) = \frac{2C_H^2}{u_k^{2H} J_{1-H}^2(u_k)}$ and $J_{1-H}^2(u_k) \sim \frac{2}{\pi u_k}$. Hence, we write-

$$\left|\sum_{k=1}^l \frac{(\sin u_k r)(\sin u_k s)}{(\mu u_k^4 + 1)^2 u_k^2}\mathrm{Var}(U_k)\right| \leq K_0 \left|\sum_{k=1}^\infty \frac{2C_H^2 \pi u_k}{2 u_k^{2+2H}}\right| < \infty$$

Thus I_{01}^l converges uniformly and absolutely to I_{01} on $[0,1]^2$ as $l \to \infty$. Similarly, we can show that I_{02}^l converges uniformly and absolutely to I_{02} on $[0,1]^2$. This implies that $Cov(G_l^H(r), G_l^H(s))$ converges to the $Cov(G_\infty^H(r), G_\infty^H(s))$ uniformly and absolutely for $(r,s) \in [0,1] \times [0,1]$. Hence the finite dimensional distributions of $\{G_l^H(r) : r \in [0,1]\}$ converge to the finite dimensional distributions of $\{G_\infty^H(r) : r \in [0,1]\}$ and this verifies step 1.

Step 2: Define, $G_l^1(r) = \sum_{k=1}^l \frac{1}{\mu u_k^4 + 1}\frac{\sin u_k r}{u_k}U_k$. Apply the maximal inequality for sub-Gaussian processes ((Van der Vaart and Wellner, 1996, Corollarly 2.2.8)) to $G_l^1(\cdot)$, giving

$$\mathbb{E} \sup_{d_l(s,t)<\delta} |G_l^1(s) - G_l^1(t)| \leq K \int_0^\delta \sqrt{\log(N(\epsilon, [0,1], d_l))}d\epsilon.$$

Here K is a universal constant, $N(\epsilon, [0,1], d_l)$ is the $\epsilon-$covering number on the semi-metric space $([0,1], d_l)$ and d_l is the standard deviation semi-metric for which

$$d_l^2(s,t) = \mathrm{Var}(G_l^1(s) - G_l^1(t)) = \sum_{k=1}^l \frac{(\sin u_k s - \sin u_k t)^2}{[u_k(1+\mu u_k^4)]^2}\sigma_u^2$$
$$\leq \sum_{k=1}^l \frac{(\sin u_k s - \sin u_k t)^2 \sigma_u^2}{u_k^2}$$
$$\leq \mathrm{Var}(B_H^l(s) - B_H^l(t))$$
$$\leq |t - s|^{2H},$$

where $\mathrm{Var}(U_k) = \sigma_u^2$. By following the proof of Dzhaparidze and Van Zanten (2004, Theorem 4.5), $G_l(\cdot)$ can be shown to be uniformly equicontinuous in probability and hence the process is asymptotically tight in $C[0,1]$. This proves step 2 of part (i). Now apply Van der Vaart and Wellner (1996, Theorem 1.5.4) which ensures that weak convergence of finite dimensional distributions combined with asymptotic tightness is sufficient for the sequence $\{G_l^H(r) : r \in [0,1]\}$ to converge weakly in $C[0,1]$, the set of continuous functions equipped with supremum metric. Finally, by a virtue of the Lévy-Ito-Nisio Proposition ((Van der Vaart and Wellner, 1996, Proposition A.1.3)) it is equivalent to convergence with probability one in $C[0,1]$ and this completes the proof of part (i).

ii. First recall from (14) that a fBM can be expressed by

$$B_H(r) = \sum_{k=1}^\infty \frac{\sin u_k r}{u_k}U_k + \sum_{k=1}^\infty \frac{1 - \cos v_k r}{v_k}V_k$$

for $r \in [0, 1]$. Since the series converges almost surely and uniformly in $r \in [0, 1]$, we define a finite series approximation

$$B_H^{K_n}(r) := \sum_{k=1}^{K_n} \frac{\sin u_k r}{u_k} U_k + \sum_{k=1}^{K_n} \frac{1 - \cos v_k r}{v_k} V_k, \tag{46}$$

where $K_n \to \infty$ as $n \to \infty$. Therefore, $\left| B_H^{K_n}(r) - B_H(r) \right| = o_{a.s.}(1)$, and then by using (22), we have,

$$\sup_{0 \le t \le n} \left| B_H^{K_n}\left(\frac{t}{n}\right) - \frac{x_t}{n^H} \right| = o_{a.s.}(1) \tag{47}$$

whenever $K_n \to \infty$ as $n \to \infty$. It follows that the HP trend solution has the approximated form as $n \to \infty$

$$
\begin{aligned}
\frac{\hat{f}_t}{n^H} &= \frac{1}{\lambda L^{-2}(1 - L)^4 + 1} \left(\frac{x_t}{n^H} \right) \\
&= \frac{1}{\lambda L^{-2}(1 - L)^4 + 1} \left[B_H^{K_n}\left(\frac{t}{n}\right) + o_{a.s}(1) \right] \\
&= \sum_{k=1}^{K_n} \left[\frac{1}{\lambda L^{-2}(1 - L)^4 + 1} \frac{\sin u_k r}{u_k} \right] U_k + \sum_{k=1}^{K_n} \left[\frac{1}{\lambda L^{-2}(1 - L)^4 + 1} \frac{1 - \cos v_k r}{v_k} \right] V_k + o_{a.s.}(1).
\end{aligned} \tag{48}
$$

As explained in PJ (2021), the $o_{a.s.}(1)$ error order in (48) holds since the two sided moving average filter generated by the operator $\frac{1}{\lambda L^{-2}(1-L)^4+1}$ is an absolutely summable weighted moving average with stable geometric decay (McElroy (2008)) which retains the error order by majorization since the errors in (20) and (47) hold uniformly for $t \le n$. Next, we find an explicit form of (48). Define

$$\psi_k\left(\frac{t}{n}\right) = \frac{\sin(u_k \frac{t}{n})}{u_k} = \frac{\mathtt{Im}(e^{iu_k \frac{t}{n}})}{u_k} \text{ and } \phi_k\left(\frac{t}{n}\right) = \frac{\cos(v_k \frac{t}{n})}{v_k} = \frac{\mathtt{Re}(e^{iv_k \frac{t}{n}})}{v_k}, \tag{49}$$

where $\mathtt{Im}\{\cdot\}$ and $\mathtt{Re}\{\cdot\}$ denote the imaginary and real parts of their complex number arguments. We write

$$
\begin{aligned}
n(1 - L)\psi_k\left(\frac{t}{n}\right) &= n\mathtt{Im}\left(\frac{e^{iu_k \frac{t}{n}}(1 - e^{-i\frac{u_k}{n}})}{u_k} \right) \\
&= \frac{\mathtt{Im}\left[e^{iu_k \frac{t}{n}}(1 - \sum_{m=0}^\infty (-i\frac{u_k}{n})^m / m!) \right]}{u_k / n} \\
&= \mathtt{Im}\left[e^{iu_k \frac{t}{n}} \left(i\left(1 + O\left(\frac{u_k^2}{n^2}\right)\right) + O\left(\frac{u_k}{n}\right) \right) \right] \\
&= u_k \mathtt{Re}\left[\frac{e^{iu_k \frac{t}{n}}}{u_k} \left(1 + O\left(\frac{u_k^2}{n^2}\right)\right) \right] + u_k \mathtt{Im}\left[\frac{e^{iu_k \frac{t}{n}}}{u_k} \left(O\left(\frac{u_k}{n}\right)\right) \right], \tag{50}
\end{aligned}
$$

uniformly for $k \leq K_n$ as $u_k, v_k = O(k)$ and $t \leq n$. Also

$$nL^{-1}(1-L)\psi_k\left(\frac{t}{n}\right) = u_k\mathrm{Re}\left[\frac{e^{iu_k(\frac{t}{n}+\frac{1}{n})}}{u_k}\left(1+O\left(\frac{u_k^2}{n^2}\right)\right)\right] + u_k\mathrm{Im}\left[\frac{e^{iu_k(\frac{t}{n}+\frac{1}{n})}}{u_k}\left(O\left(\frac{u_k}{n}\right)\right)\right]$$

$$= u_k\mathrm{Re}\left[\frac{e^{iu_k\frac{t}{n}}}{u_k}\left(1+O\left(\frac{u_k^2}{n^2}\right)\right)\right] + u_k\mathrm{Im}\left[\frac{e^{iu_k\frac{t}{n}}}{u_k}\left(O\left(\frac{u_k}{n}\right)\right)\right].$$

Similarly,

$$nL^{-1}(1-L)\phi_k\left(\frac{t}{n}\right) = -v_k\mathrm{Im}\left[\frac{e^{iv_k\frac{t}{n}}}{v_k}\left(1+O\left(\frac{v_k^2}{n^2}\right)\right)\right] + v_k\mathrm{Re}\left[\frac{e^{iv_k\frac{t}{n}}}{v_k}\left(O\left(\frac{v_k}{n}\right)\right)\right],$$

uniformly for all $k \leq K_n$ and $t \leq n$. Since $\frac{d}{dr}\left(\frac{\sin u_l r}{u_l}\right) = \cos u_l r$, the operator $n(1-L)$ applied to $\psi_k\left(\frac{t}{n}\right)$ acts asymptotically like the differential operator $D = \frac{d}{dr}$ on $\psi_k\left(\frac{t}{n}\right)$ as $\frac{K_n}{n} \to 0$ with $n \to \infty$ and L^{-1} acts like an identity operator asymptotically. By repeating the above steps, we find that

$$n^2(1-L)^2\psi_k\left(\frac{t}{n}\right) = n(1-L)n(1-L)\psi_k\left(\frac{t}{n}\right)$$

$$= n(1-L)\left\{\mathrm{Re}\left[e^{iu_k\frac{t}{n}}\left(1+O\left(\frac{u_k^2}{n^2}\right)\right)\right] + \mathrm{Im}\left[e^{iu_k\frac{t}{n}}\left(O\left(\frac{u_k}{n}\right)\right)\right]\right\}$$

$$= u_k\mathrm{Re}\left(\frac{e^{iu_k\frac{t}{n}}(1-e^{-i\frac{u_k}{n}})}{u_k/n}\right)\left(1+O\left(\frac{u_k^2}{n^2}\right)\right)$$

$$+ u_k\mathrm{Im}\left(\frac{e^{iu_k\frac{t}{n}}(1-e^{-i\frac{u_k}{n}})}{u_k/n}\right)O\left(\frac{u_k}{n}\right)$$

$$= u_k\mathrm{Re}\left[e^{iu_k\frac{t}{n}}\left(i\left(1+O\left(\frac{u_k^2}{n^2}\right)\right)+O\left(\frac{u_k}{n}\right)\right)\right]\left(1+O\left(\frac{u_k^2}{n^2}\right)\right)$$

$$+ u_k\mathrm{Im}\left[e^{iu_k\frac{t}{n}}\left(i\left(1+O\left(\frac{u_k^2}{n^2}\right)\right)+O\left(\frac{u_k}{n}\right)\right)\right]O\left(\frac{u_k}{n}\right)$$

$$= -u_k\mathrm{Im}\left[e^{iu_k\frac{t}{n}}\left(1+O\left(\frac{u_k^2}{n^2}\right)\right)\right] + u_k\mathrm{Re}\left[e^{iu_k\frac{t}{n}}\left(O\left(\frac{u_k}{n}\right)\right)\right]$$

$$= -u_k^2\mathrm{Im}\left[\frac{e^{iu_k\frac{t}{n}}}{u_k}\left(1+O\left(\frac{u_k^2}{n^2}\right)\right)\right] + u_k^2\mathrm{Re}\left[\frac{e^{iu_k\frac{t}{n}}}{u_k}\left(O\left(\frac{u_k}{n}\right)\right)\right].$$

Hence recursively, we obtain

$$n^4(1-L)^4\psi_k\left(\frac{t}{n}\right) = u_k^4\mathrm{Im}\left[\frac{e^{iu_k\frac{t}{n}}}{u_k}\left(1+O\left(\frac{u_k^2}{n^2}\right)\right)\right] + u_k^4\mathrm{Re}\left[\frac{e^{iu_k\frac{t}{n}}}{u_k}\left(O\left(\frac{u_k}{n}\right)\right)\right],$$

uniformly for $k \leq K_n$. Further,

$$n^4L^{-2}(1-L)^4\psi_k\left(\frac{t}{n}\right) = u_k^4\mathrm{Im}\left[\frac{e^{iu_k(\frac{t}{n}+\frac{2}{n})}}{u_k}\left(1+O\left(\frac{u_k^2}{n^2}\right)\right)\right] + u_k^4\mathrm{Re}\left[\frac{e^{iu_k(\frac{t}{n}+\frac{2}{n})}}{u_k}\left(O\left(\frac{u_k}{n}\right)\right)\right]$$

$$= u_k^4 \text{Im} \left[\frac{e^{iu_k \frac{t}{n}}}{u_k} \left(1 + O\left(\frac{u_k^2}{n^2} \right) \right) \right] + u_k^4 \text{Re} \left[\frac{e^{iu_k \frac{t}{n}}}{u_k} \left(O\left(\frac{u_k}{n} \right) \right) \right]$$

$$= u_k^4 \text{Im} \left[\frac{e^{iu_k \frac{t}{n}}}{u_k} \left(1 + O\left(\frac{K_n^2}{n^2} \right) \right) \right] + u_k^4 \text{Re} \left[\frac{e^{iu_k \frac{t}{n}}}{u_k} \left(O\left(\frac{K_n}{n} \right) \right) \right].$$

$$(51)$$

The last line in (51) is explained by noting that $u_k = O(k)$ and $k \leq K_n$. Using (51), for any $l \in \mathbb{N}$, we can write iteratively

$$[n^4 L^{-2} (1-L)^4]^l \psi_k \left(\frac{t}{n} \right) = u_k^{4l} \text{Im} \left[\frac{e^{iu_k \frac{t}{n}}}{u_k} \left(1 + O\left(\frac{K_n^2}{n^2} \right) \right) \right] + u_k^{4l} \text{Re} \left[\frac{e^{iu_k \frac{t}{n}}}{u_k} \left(O\left(\frac{K_n}{n} \right) \right) \right],$$

$$(52)$$

uniformly for $k \leq K_n$ and $0 \leq t \leq n$. Similarly, we have

$$[n^4 L^{-2} (1-L)^4]^l \phi_k \left(\frac{t}{n} \right) = v_k^{4l} \text{Re} \left[\frac{e^{iv_k \frac{t}{n}}}{v_k} \left(1 + O\left(\frac{K_n^2}{n^2} \right) \right) \right] + v_k^{4l} \text{Im} \left[\frac{e^{iv_k \frac{t}{n}}}{v_k} \left(O\left(\frac{K_n}{n} \right) \right) \right],$$

$$(53)$$

uniformly for $k \leq K_n$ and $0 \leq t \leq n$. Now, the operations in square parentheses in (48) can be evaluated as follows

$$\frac{1}{\lambda L^{-2} (1-L)^4 + 1} \psi_k \left(\frac{t}{n} \right)$$

$$= \int_0^\infty \exp\{-(\lambda L^{-2}(1-L)^4 + 1)s\} ds \, \psi_k \left(\frac{t}{n} \right)$$

$$= \int_0^\infty e^{-s} \sum_{l=0}^\infty \frac{(-\mu n^4 L^{-2}(1-L)^4 s)^l}{l!} \psi_k \left(\frac{t}{n} \right) ds, \quad \lambda = \mu n^4$$

$$= \int_0^\infty e^{-s} \sum_{l=0}^\infty \frac{(-\mu s)^l u_k^{4l}}{l!} \left\{ \text{Im} \left[\frac{e^{iu_k \frac{t}{n}}}{u_k} \left(1 + O\left(\frac{K_n^2}{n^2} \right) \right) \right] + \text{Re} \left[\frac{e^{iu_k \frac{t}{n}}}{u_k} \left(O\left(\frac{K_n}{n} \right) \right) \right] \right\} ds$$

$$= \int_0^\infty e^{-s - \mu u_k^4 s} ds \left\{ \text{Im} \left[\frac{e^{iu_k \frac{t}{n}}}{u_k} \left(1 + O\left(\frac{K_n^2}{n^2} \right) \right) \right] + \text{Re} \left[\frac{e^{iu_k \frac{t}{n}}}{u_k} \left(O\left(\frac{K_n}{n} \right) \right) \right] \right\}$$

$$= \frac{1}{\mu u_k^4 + 1} \left\{ \text{Im} \left[\frac{e^{iu_k \frac{t}{n}}}{u_k} \left(1 + O\left(\frac{K_n^2}{n^2} \right) \right) \right] + \text{Re} \left[\frac{e^{iu_k \frac{t}{n}}}{u_k} \left(O\left(\frac{K_n}{n} \right) \right) \right] \right\},$$

$$(54)$$

where the third equality above follows from (52). By iterating previous steps on ϕ_k, we obtain,

$$\frac{1}{\lambda L^{-2} (1-L)^4 + 1} \phi_k \left(\frac{t}{n} \right)$$

$$= \frac{1}{\mu v_k^4 + 1} \left\{ \text{Re} \left[\frac{e^{iv_k \frac{t}{n}}}{v_k} \left(1 + O\left(\frac{K_n^2}{n^2} \right) \right) \right] + \text{Im} \left[\frac{e^{iv_k \frac{t}{n}}}{v_k} \left(O\left(\frac{K_n}{n} \right) \right) \right] \right\}$$

$$(55)$$

uniformly for $k \leq K_n$. Also, $\frac{1}{\lambda L^{-2}(1-L)^4+1}\frac{1}{v_k} = \frac{1}{u_k}$ for all $k \in \mathbb{N}$, as v_k is a constant. Now, (54), (55), and the representation of $B_H^{K_n}$ in (46) imply that

$$
\frac{1}{\lambda L^{-2}(1-L)^4+1} B_H^{K_n}\left(\frac{t}{n}\right)
$$

$$
= \sum_{k=1}^{K_n} \frac{1}{\lambda L^{-2}(1-L)^4+1}\left[\psi_k\left(\frac{t}{n}\right)U_k + \left(\frac{1}{v_k} - \phi_k\left(\frac{t}{n}\right)\right)V_k\right]
$$

$$
= \sum_{k=1}^{K_n} \frac{1}{\mu u_k^4+1}\left\{ \mathrm{Im}\left[\frac{e^{iu_k\frac{t}{n}}}{u_k}\left(1+O\left(\frac{K_n^2}{n^2}\right)\right)\right] + \mathrm{Re}\left[\frac{e^{iu_k\frac{t}{n}}}{u_k}\left(O\left(\frac{K_n}{n}\right)\right)\right]\right\}U_k
$$

$$
+ \sum_{k=1}^{K_n}\left[\frac{1}{v_k} - \frac{1}{\mu v_k^4+1}\left\{\mathrm{Re}\left[\frac{e^{iv_k\frac{t}{n}}}{v_k}\left(1+O\left(\frac{K_n^2}{n^2}\right)\right)\right] + \mathrm{Im}\left[\frac{e^{iv_k\frac{t}{n}}}{v_k}\left(O\left(\frac{K_n}{n}\right)\right)\right]\right\}\right]V_k
$$

$$
:= I_1 + I_2.
$$

Next, we need to show the series in I_1 and I_2 converge uniformly and almost surely as $K_n, n \to \infty$ and $\frac{K_n}{n} \to 0$. Hence, we can ignore the terms of $O\left(\frac{K_n^2}{n^2}\right)$ and since $u_k = O(k)$, I_1 can be reduced to

$$
I_1 = \sum_{k=1}^{K_n} \frac{1}{\mu u_k^4+1}\frac{\sin u_k\frac{t}{n}}{u_k}U_k + \sum_{k=1}^{K_n} \frac{1}{1+\mu u_k^4}\frac{1}{u_k}O\left(\frac{K_n}{n}\right)U_k
$$

$$
= \sqrt{2}\sum_{k=1}^{K_n} \frac{1}{\mu u_k^4+1}\frac{\sin u_k\frac{t}{n}}{u_k}C_H u_k^{-H}J_{1-H}^{-1}(u_k)U_k'
$$

$$
+ \sqrt{2}\,O\left(\frac{K_n}{n}\right)\sum_{k=1}^{K_n} \frac{1}{1+\mu u_k^4}\frac{1}{u_k}C_H u_k^{-H}J_{1-H}^{-1}(u_k)U_k'
$$

$$
:= I_{11} + O\left(\frac{K_n}{n}\right)I_{12},
$$

where we replaced U_k by $\sqrt{2}C_H u_k^{-H}J_{1-H}^{-1}(u_k)U_k'$ and U_k' is a standard normal random variable, see (13). The u_k are the roots of J_{-H}. Hence, by using the property, $J_v^2(z) + J_{v+1}^2(z) \sim \frac{2}{\pi z}$ for large z and choosing $v = -H$, we get $J_{1-H}^2(u_k) \sim \frac{2}{\pi u_k}$. This leads to $\mathbb{E}|I_{12}| \leq C\sum_{k=1}^{K_n} \frac{1}{1+\mu u_k^4}\frac{1}{u_k^{1+H-1/2}} < \infty$ for some constant $C > 0$, since $u_k = O(k)$. Therefore, $I_{12} < \infty$ almost everywhere for $H \in (0,1)$. Similarly, $\mathbb{E}|I_{11}| \leq \mathbb{E}|I_{12}| < \infty$ which implies that $I_{11} < \infty$ almost every-where. Hence, combining I_{11} and I_{12}, we get,

$$
I_1 = \sum_{k=1}^{K_n} \frac{1}{\mu u_k^4+1}\frac{\sin u_k\frac{t}{n}}{u_k}U_k + O_{a.s.}\left(\frac{K_n}{n}\right). \tag{56}
$$

For I_2, we decompose the series as

$$
I_2 = \sum_{k=1}^{K_n} \frac{V_k}{v_k} - \sum_{k=1}^{K_n} \frac{1}{1+\mu v_k^4}\frac{\cos v_k\frac{t}{n}}{v_k}V_k + O\left(\frac{K_n}{n}\right) \times \sum_{k=1}^{K_n} \frac{1}{1+\mu v_k^4}\frac{1}{v_k}V_k
$$

$$:= I_{21} + I_{22} + I_{23} \times O\left(\frac{K_n}{n}\right).$$

Now

$$\text{Var}(I_{21}) = \sum_{k=1}^{K_n} \frac{2C_H^2 v_k^{-2H} J_{-H}^{-2}(v_k)}{v_k^2} < C \sum_{k=1}^{K_n} \frac{C_H^2 v_k^{-2H} \pi v_k}{v_k^2} < \infty \text{ for some constant } C$$

if $K_n \to \infty$ as $n \to \infty$. Thus, $I_{21}^{K_n} := I_{21}$ is an L^2 bounded martingale with respect to the natural filtration. Hence, by the martingale convergence theorem $I_{21}^{K_n}$ converges a.s. to $\sum_{k=1}^{\infty} \frac{V_k}{v_k}$ as $K_n \to \infty$. By applying the same method as used to show the convergence of I_{11} and I_{12}, the convergence of I_{22} and I_{23} can be established. Hence, we get,

$$I_2 = \sum_{k=1}^{K_n} \frac{V_k}{v_k} - \sum_{k=1}^{K_n} \frac{1}{1 + \mu v_k^4} \frac{\cos v_k \frac{t}{n}}{v_k} V_k + O_{a.s.}\left(\frac{K_n}{n}\right), \tag{57}$$

for all $K_n \in \mathbb{N}$. By combining (56) and (57), we write,

$$\frac{1}{\mu n^4 L^{-2}(1-L)^4 + 1} B_H^{K_n}\left(\frac{t}{n}\right) = \sum_{k=1}^{K_n} \frac{1}{\mu u_k^4 + 1} \frac{\sin u_k \frac{t}{n}}{u_k} U_k + \sum_{k=1}^{K_n} \left[\frac{1}{v_k} - \frac{1}{1 + \mu v_k^4} \frac{\cos v_k \frac{t}{n}}{v_k}\right] V_k$$
$$+ O_{a.s.}\left(\frac{K_n}{n}\right) \tag{58}$$

for $H \in (0,1)$. Finally, (48) and (58) together show that

$$\frac{\hat{f}_{K_n}^{HP}(t)}{n^H} = \left[\sum_{k=1}^{K_n} \frac{1}{\mu u_k^4 + 1} \frac{\sin u_k r}{u_k} U_k + \sum_{k=1}^{K_n} \left(\frac{1}{v_k} - \frac{1}{\mu v_k^4 + 1} \frac{\cos v_k r}{v_k}\right) V_k\right] + O_{a.s.}\left(\frac{K_n}{n}\right) + o(1).$$

Therefore, the continuous limit form of the HP filter applied to the stochastic trend x_t is

$$G_\infty^H(r) = \sum_{k=1}^{\infty} \frac{1}{\mu u_k^4 + 1} \frac{\sin u_k r}{u_k} U_k + \sum_{k=1}^{\infty} \left[\frac{1}{v_k} - \frac{1}{\mu v_k^4 + 1} \frac{\cos v_k r}{v_k}\right] V_k$$

provided $K_n \to \infty$, $\frac{K_n}{n} \to 0$ as $n \to \infty$. This yields the desired results in (27) and (28).

Proof of remark 3.5: For a sequence $\{\mu_L\}_{L=1}^{\infty}$, we obtained from the proof of Theorem 3.1,

$$\frac{\hat{f}_{K_n}^{HP}(t)}{n^H} = \left[\sum_{k=1}^{K_n} \frac{1}{\mu_L u_k^4 + 1} \frac{\sin u_k r}{u_k} U_k + \sum_{k=1}^{K_n} \left(\frac{1}{v_k} - \frac{1}{\mu_L v_k^4 + 1} \frac{\cos v_k r}{v_k}\right) V_k\right] + O_{a.s.}\left(\frac{K_n}{n}\right) + o(1).$$

We have $u_k, v_k = O(k)$, so that for any K_n, both $\mu_L u_k^4, \mu_L v_k^4 \to 0$ uniformly as $K_n^4 \mu_L \to 0$. Thus, taking $K_n \to \infty$ as $n \to \infty$ such that $\frac{K_n}{n} \to 0$ followed by $\mu_L \to 0$ as $L \to \infty$ gives the result.

Proof of Theorem 4.1: Since x_t satisfies the functional law (22), we can write

$$(1 - S_n^\lambda)^{\mathrm{m}} \frac{x_{\lfloor nr \rfloor}}{n^H} = (1 - S_n^\lambda)^{\mathrm{m}} B_H(r) + o(1) = (1 - S_n^\lambda)^{\mathrm{m}} B_H^{K_n}(r) + o(1), \tag{59}$$

where $B_H^{K_n}(r)$ is the finite series approximation of $B_H(r)$ given by (46) and $S_n^\lambda = \frac{1}{1+\mu n^4 L^{-2}(1-L)^2}$ with $\lambda = \mu n^4$. We further write,

$$(1 - S_n^\lambda)^m B_H^{K_n}\left(\frac{t}{n}\right) = \left(\frac{\mu n^4 L^{-2}(1-L)^4}{1+\mu n^4 L^{-2}(1-L)^4}\right)^m \left[\sum_{k=1}^{K_n} \frac{\sin u_k \frac{t}{n}}{u_k} U_k + \sum_{k=1}^{K_k} \frac{1 - \cos v_k \frac{t}{n}}{v_k} V_k\right]$$

$$= \left(\frac{\mu n^4 L^{-2}(1-L)^4}{1+\mu n^4 L^{-2}(1-L)^4}\right)^m \sum_{k=1}^{K_n} \psi_k\left(\frac{t}{n}\right) U_k$$

$$+ \left(\frac{\mu n^4 L^{-2}(1-L)^4}{1+\mu n^4 L^{-2}(1-L)^4}\right)^m \sum_{k=1}^{K_n} \left(\frac{1}{v_k} - \phi_k\left(\frac{t}{n}\right)\right) V_k$$

$$:= I_3 + I_4,$$

where ψ and ϕ are defined by (49). Now, we claim that I_3 and I_4 can be written as

$$I_3 = \sum_{k=1}^{K_n} \frac{\mu^m u_k^{4m}}{(\mu u_k^4 + 1)^m} \texttt{Im}\left(\frac{e^{iu_k \frac{t}{n}}}{u_k}\right) U_k + O_{a.s.}\left(\frac{K_n}{n}\right), \tag{60}$$

and

$$I_4 = -\sum_{k=1}^{K_n} \frac{\mu^m v_k^{4m}}{(\mu v_k^4 + 1)^m} \texttt{Im}\left(\frac{e^{iv_k \frac{t}{n}}}{v_k}\right) V_k + O_{a.s.}\left(\frac{K_n}{n}\right), \tag{61}$$

respectively. Combining (60) and (61), we see that

$$(1 - S_n^\lambda)^m B_H^{K_n}\left(\frac{t}{n}\right) = \sum_{k=1}^{K_n} \frac{\mu^m u_k^{4m}}{(\mu u_k^4 + 1)^m} \texttt{Im}\left(\frac{e^{iu_k \frac{t}{n}}}{u_k}\right) U_k - \sum_{k=1}^{K_n} \frac{\mu^m v_k^{4m}}{(\mu v_k^4 + 1)^m} \texttt{Im}\left(\frac{e^{iv_k \frac{t}{n}}}{v_k}\right) V_k$$

$$+ O_{a.s.}\left(\frac{K_n}{n}\right), \tag{62}$$

for $H \in (0, 1)$. Recall that by applying the HP filter m times, we have the estimated cycle and trend as

$$\frac{\hat{c}_t^{(m)}}{n^H} = (1 - S_n^\lambda)^m \frac{x_t}{n^H}, \tag{63}$$

and

$$\frac{\hat{f}_t^{(m)}}{n^H} = (1 - (1 - S_n^\lambda)^m) \frac{x_t}{n^H} = (1 - (1 - S_n^\lambda)^m) B_H^{K_n}(r) + o_{a.s.}(1), \tag{64}$$

respectively. Now, if $(1 - S_n^\lambda)^m B_H^{K_n}(r)$ tends to zero a.s., then $\frac{\hat{f}_{\lfloor nr \rfloor}^m}{n^H} \to B_H(r)$, giving the desired result. To see this, first note that $\left(\frac{\mu(iu_k)^4}{1+\mu(iu_k)^4}\right)^m \leq \left(1 + \frac{1}{\mu u_{K_n}^4}\right)^{-m}$ for all $u_1 < u_2 < \cdots < u_{K_n}$ and $0 \leq k \leq K_n$. The upper bound $\left(1 + \frac{1}{\mu u_{K_n}^4}\right)^{-m}$ tends to zero if and only if $-m \log(1 + \frac{1}{\mu u_{K_n}^4}) \to -\infty$. Now $-m \log(1 + \frac{1}{\mu u_{K_n}^4}) \to \infty$ if $\frac{m}{u_{K_n}^4} \to \infty$ as $K_n \to \infty$. Similarly, $\left(\frac{\mu(iv_k)^4}{1+\mu(iv_k)^4}\right)^m \to 0$, as $\frac{m}{v_{K_n}^4} \to \infty$. Therefore, the LHS in (62) tends to zero if $\frac{K_n^4}{m}, \frac{K_n}{n} \to 0$ as $n \to \infty$. Consequently,

from (63) and (64) $\frac{\hat{c}_t^{\mathrm{m}}}{n^H} = 0$ and $\frac{\hat{f}_t^{\mathrm{m}}}{n^H} \to B_H(t)$ almost surely and this completes the proof of the main results of the Theorem. It remains to prove the claims in (60) and (61) by using a technique similar to the derivation of (52) and (53). First, note that

$$
\left(\frac{\mu n^4 L^{-2}(1-L)^4}{1+\mu n^4 L^{-2}(1-L)^4} \right)^{\mathrm{m}} \psi_k\left(\frac{t}{n} \right)
$$

$$
= (\mu n^4 L^{-2}(1-L)^4)^{\mathrm{m}} \int_0^\infty \frac{e^{-(1+\mu n^4 L^{-2}(1-L)^4)s} s^{\mathrm{m}-1}}{(\mathrm{m}-1)!} \psi_k\left(\frac{t}{n} \right) ds
$$

$$
= \frac{(\mu n^4 L^{-2}(1-L)^4)^{\mathrm{m}}}{(\mathrm{m}-1)!} \int_0^\infty e^{-s} s^{\mathrm{m}-1} \sum_{l=0}^\infty (-s\mu n^4 L^{-2}(1-L)^4)^l \psi_k\left(\frac{t}{n} \right) ds
$$

$$
= \frac{1}{(\mathrm{m}-1)!} \int_0^\infty e^{-s} s^{\mathrm{m}-1} \sum_{l=0}^\infty \frac{(-s)^l (\mu n^4 L^{-2}(1-L)^4)^{l+\mathrm{m}}}{l!} \psi_k\left(\frac{t}{n} \right) ds
$$

$$
= \frac{1}{(\mathrm{m}-1)!} \int_0^\infty e^{-s} s^{\mathrm{m}-1} \sum_{l=0}^\infty \frac{(-s)^l (\mu u_k^4)^{(l+\mathrm{m})}}{l!} ds
$$

$$
\times \left\{ \mathrm{Im}\left[\frac{e^{iu_k \frac{t}{n}}}{u_k} \left(1 + O\left(\frac{K_n^2}{n^2} \right) \right) \right] + \mathrm{Re}\left[\frac{e^{iu_k \frac{t}{n}}}{u_k} \left(O\left(\frac{K_n}{n} \right) \right) \right] \right\} ds
$$

$$
= \frac{\mu^{\mathrm{m}} u_k^{4\mathrm{m}}}{(\mathrm{m}-1)!} \left\{ \mathrm{Im}\left[\frac{e^{iu_k \frac{t}{n}}}{u_k} \left(1 + O\left(\frac{K_n^2}{n^2} \right) \right) \right] + \mathrm{Re}\left[\frac{e^{iu_k \frac{t}{n}}}{u_k} \left(O\left(\frac{K_n}{n} \right) \right) \right] \right\}
$$

$$
\times \int_0^\infty e^{-s} s^{\mathrm{m}-1} \sum_{l=0}^\infty \frac{(-s\mu)^l u_k^{4l}}{l!} ds
$$

$$
= \frac{\mu^{\mathrm{m}} u_k^{4\mathrm{m}}}{(\mathrm{m}-1)!} \left\{ \mathrm{Im}\left[\frac{e^{iu_k \frac{t}{n}}}{u_k} \left(1 + O\left(\frac{K_n^2}{n^2} \right) \right) \right] + \mathrm{Re}\left[\frac{e^{iu_k \frac{t}{n}}}{u_k} \left(O\left(\frac{K_n}{n} \right) \right) \right] \right\}
$$

$$
\times \int_0^\infty e^{-s-s\mu u_k^4} s^{\mathrm{m}-1} ds
$$

$$
= \frac{\mu^{\mathrm{m}} u_k^{4\mathrm{m}}}{(\mu u_k^4 + 1)^{\mathrm{m}}} \left\{ \mathrm{Im}\left[\frac{e^{iu_k \frac{t}{n}}}{u_k} \left(1 + O\left(\frac{K_n^2}{n^2} \right) \right) \right] + \mathrm{Re}\left[\frac{e^{iu_k \frac{t}{n}}}{u_k} \left(O\left(\frac{K_n}{n} \right) \right) \right] \right\}.
$$

Hence I_3 can be written as

$$
I_3 = \sum_{k=1}^{K_n} \frac{\mu^{\mathrm{m}} u_k^{4\mathrm{m}}}{(\mu u_k^4 + 1)^{\mathrm{m}}} \left\{ \mathrm{Im}\left[\frac{e^{iu_k \frac{t}{n}}}{u_k} \left(1 + O\left(\frac{K_n^2}{n^2} \right) \right) \right] + \mathrm{Re}\left[\frac{e^{iu_k \frac{t}{n}}}{u_k} \left(O\left(\frac{K_n}{n} \right) \right) \right] \right\} U_k.
$$

We need to show that I_3 converges as $n, K_n \to \infty$ and $\frac{K_n}{n} \to 0$. Following a similar argument to the finiteness of $\sum_{k=1}^{K_n} \frac{V_k}{v_k} < \infty$ in Theorem 3.1 it can be shown that $\sum_{k=1}^{K_n} \frac{U_k}{u_k} < \infty$ with probability 1 as $K_n \to \infty$. Moreover,

$$
\mathrm{Var}\left(\sum_{k=1}^{K_n} \frac{\mu^{\mathrm{m}} u_k^{4\mathrm{m}}}{(\mu u_k^4 + 1)^{\mathrm{m}}} \mathrm{Im}\left(\frac{e^{iu_k \frac{t}{n}}}{u_k} \right) U_k \right) < \mathrm{Var}\left(\sum_{k=1}^{K_n} \frac{U_k}{u_k} \right) < \infty,
$$

and

$$\text{Var}\left(\sum_{k=1}^{K_n} \frac{\mu^{\text{m}} u_k^{4\text{m}}}{(\mu u_k^4 + 1)^{\text{m}}} \left(\frac{U_k}{u_k}\right)\right) < \text{Var}\left(\sum_{k=1}^{K_n} \frac{U_k}{u_k}\right) < \infty.$$

Using the martingale convergence theorem as in the convergence of I_{21} in the proof of Theorem 3.1, the sums in I_3 can be shown to be finite a.s. for $H \in (0,1)$ as $K_n \to \infty$, giving $O\left(\frac{K_n}{n}\right) \times \sum_{k=1}^{K_n} \frac{\mu^{\text{m}} u_k^{4\text{m}}}{(\mu u_k^4 + 1)^{\text{m}}} \frac{U_k}{u_k} = O_{a.s.}\left(\frac{K_n}{n}\right)$. Therefore, I_3 can be written as

$$I_3 = \sum_{k=1}^{K_n} \frac{\mu^{\text{m}} u_k^{4\text{m}}}{(\mu u_k^4 + 1)^{\text{m}}} \text{Im}\left(\frac{e^{iu_k \frac{t}{n}}}{u_k}\right) U_k + O_{a.s.}\left(\frac{K_n}{n}\right), \tag{65}$$

which proves the claim in (60). Next, we need to compute I_4. The ratio $\frac{V_k}{v_k}$ does not depend on t so that $(1 - L)\frac{V_k}{v_k} = 0$ and hence

$$\left(\frac{\mu n^4 L^{-2}(1 - L)^4}{1 + \mu n^4 L^{-2}(1 - L)^4}\right)^{\text{m}} \frac{V_k}{v_k} = 0,$$

giving $I_4 = -\left(\frac{\mu n^4 L^{-2}(1-L)^4}{1+\mu n^4 L^{-2}(1-L)^4}\right)^{\text{m}} \sum_{k=1}^{K_n} \phi_k\left(\frac{t}{n}\right) V_k$. Next, by using the same method as used to compute I_3, we obtain

$$I_4 = -\sum_{k=1}^{K_n} \frac{\mu^{\text{m}} v_k^{4\text{m}}}{(\mu v_k^4 + 1)^{\text{m}}} \text{Im}\left(\frac{e^{iv_k \frac{t}{n}}}{v_k}\right) V_k + O_{a.s.}\left(\frac{K_n}{n}\right), \tag{66}$$

which yields the claim in (61).

Proof of Proposition 4.4:
We have $(1 - (1 - S_n^\lambda)^{\text{m}})\frac{y_{t=\lfloor nr \rfloor}}{n^H} = (1 - (1 - S_n^\lambda)^{\text{m}})\frac{g_n(\lfloor nr \rfloor)}{n^H} + (1 - (1 - S_n^\lambda)^{\text{m}})\frac{x_{\lfloor nr \rfloor}}{n^H}$. Theorem 4.1 shows that $(1 - (1 - S_n^\lambda)^{\text{m}})\frac{x_{\lfloor nr \rfloor}}{n^H} \xrightarrow{a.s} B_H(r)$ and it remains to show

$$(1 - (1 - S_n^\lambda)^{\text{m}})\frac{g_{\lfloor nr \rfloor}}{n^H} \to g(r), \tag{67}$$

as $n \to \infty$. Note that $\frac{g_n(r)}{n^H} = g(r) + o(1)$ and it follows that

$$\left[1 - \left(1 - S_n^\lambda\right)^m\right] \frac{g_n\left(\frac{t}{n}\right)}{n^H} = \left[1 - \left(1 - S_n^\lambda\right)^m\right] g\left(\frac{t}{n}\right) + o(1). \tag{68}$$

To get the desired result (67) we show that

$$\left[1 - \left(1 - S_n^\lambda\right)^m\right] g\left(\frac{t}{n}\right) \to g(r) \tag{69}$$

as $n \to \infty$. Write

$$g\left(\frac{t}{n}\right) = \alpha_o + \sum_{k=1}^{M} \alpha_k \text{Im}(e^{i2\pi k \frac{t}{n}}) + \sum_{k=1}^{M} \beta_k \text{Re}(e^{i2\pi k \frac{t}{n}}), \tag{70}$$

and

$$n(1-L)g\left(\frac{t}{n}\right) = n\left[\sum_{k=1}^{M}\alpha_k\mathrm{Im}(e^{2i\pi k\frac{t}{n}}(1-e^{-2i\pi k\frac{1}{n}})) + \sum_{k=1}^{M}\beta_k\mathrm{Re}(e^{2i\pi k\frac{t}{n}}(1-e^{-2i\pi k\frac{1}{n}}))\right]. \quad (71)$$

Using $1 - e^{-2i\pi k\frac{1}{n}} = 2i\pi kn^{-1} + O\left(\frac{k^2}{n^2}\right)$, we can rewrite (71) as

$$
\begin{aligned}
n(1-L)g\left(\frac{t}{n}\right) = &\sum_{k=1}^{M}\alpha_k\mathrm{Im}\left(e^{2i\pi k\frac{t}{n}}\left(2i\pi k + O\left(\frac{k^2}{n}\right)\right)\right)\\
&+ \sum_{k=1}^{M}\beta_k\mathrm{Re}\left(e^{2i\pi k\frac{t}{n}}\left(2i\pi k + O\left(\frac{k^2}{n}\right)\right)\right).
\end{aligned} \quad (72)
$$

We also have

$$
\begin{aligned}
nL^{-2}(1-L)g\left(\frac{t}{n}\right) &= \sum_{k=1}^{M}\alpha_k\mathrm{Im}\left(e^{2i\pi k\frac{t}{n}}\left(2i\pi k + O\left(\frac{k^2}{n}\right)\right)\right)\\
&+ \sum_{k=1}^{M}\beta_k\mathrm{Re}\left(e^{2i\pi k\frac{t}{n}}\left(2i\pi k + O\left(\frac{k^2}{n}\right)\right)\right)\\
&= \sum_{k=1}^{M}\alpha_k(2\pi k)\mathrm{Im}\left[e^{2i\pi k\frac{t}{n}}\left(i + O\left(\frac{k}{n}\right)\right)\right]\\
&+ \sum_{k=1}^{M}\beta_k(2\pi k)\mathrm{Re}\left[e^{2i\pi k\frac{t}{n}}\left(i + O\left(\frac{k}{n}\right)\right)\right].
\end{aligned}
$$

Similarly,

$$
\begin{aligned}
n^2L^{-2}(1-L)^2g\left(\frac{t}{n}\right) &= \sum_{k=1}^{M}\alpha_k(2\pi k)^2\mathrm{Im}\left[e^{2i\pi k\frac{t}{n}}\left(i + O\left(\frac{k}{n}\right)\right)\left(i + O\left(\frac{k}{n}\right)\right)\right]\\
&+ \sum_{k=1}^{M}\beta_k(2\pi k)^2\mathrm{Re}\left[e^{2i\pi k\frac{t}{n}}\left(i + O\left(\frac{k}{n}\right)\right)\left(i + O\left(\frac{k}{n}\right)\right)\right]\\
&= \sum_{k=1}^{M}\alpha_k(2\pi k)^2\left[\mathrm{Im}\left(i^2 e^{2i\pi k\frac{t}{n}}\right) + O\left(\frac{k}{n}\right)\right]\\
&+ \sum_{k=1}^{M}\beta_k(2\pi k)^2\left[\mathrm{Re}\left(i^2 e^{2i\pi k\frac{t}{n}}\right) + O\left(\frac{k}{n}\right)\right],
\end{aligned}
$$

and

$$n^4L^{-2}(1-L)^4g\left(\frac{t}{n}\right) = \sum_{k=1}^{M}\alpha_k(2\pi k)^4\left[\mathrm{Im}\left(e^{2i\pi k\frac{t}{n}}\right) + O\left(\frac{k}{n}\right)\right]$$

$$+ \sum_{k=1}^{M} \beta_k (2\pi k)^4 \left[\text{Re} \left(e^{2i\pi k \frac{t}{n}} \right) + O\left(\frac{k}{n} \right) \right].$$

Therefore, for any general $l \in \mathbb{N}$, we obtain

$$(n^4 L^{-2}(1-L)^4)^l g\left(\frac{t}{n} \right) = \sum_{k=1}^{M} \alpha_k (2\pi k)^{4l} \left[\text{Im} \left(e^{2i\pi k \frac{t}{n}} \right) + O\left(\frac{k}{n} \right) \right]$$

$$+ \sum_{k=1}^{M} \beta_k (2\pi k)^{4l} \left[\text{Re} \left(e^{2i\pi k \frac{t}{n}} \right) + O\left(\frac{k}{n} \right) \right].$$

Next, computing (68) we have

$$(1 - S_n^\lambda)^{\text{m}} g\left(\frac{t}{n} \right) = (\mu n^4 L^{-2}(1-L)^4)^{\text{m}} \int_0^\infty \frac{e^{-(1+\mu n^4 L^{-2}(1-L)^4)s} s^{\text{m}-1}}{(\text{m}-1)!} g\left(\frac{t}{n} \right) ds$$

$$= \frac{(\mu n^4 L^{-2}(1-L)^4)^{\text{m}}}{(\text{m}-1)!} \int_0^\infty e^{-s} s^{\text{m}-1} \sum_{l=0}^{\infty} \frac{(-s\mu n^4 L^{-2}(1-L)^4)^l}{l!} g\left(\frac{t}{n} \right) ds$$

$$= \frac{1}{(\text{m}-1)!} \int_0^\infty e^{-s} s^{\text{m}-1} \sum_{l=0}^{\infty} \frac{(-s)^l (\mu n^4 L^{-2}(1-L)^4)^{l+\text{m}}}{l!} g\left(\frac{t}{n} \right) ds$$

$$= \sum_{k=1}^{M} \frac{\alpha_k}{(\text{m}-1)!} \int_0^\infty e^{-s} s^{\text{m}-1} \sum_{l=0}^{\infty} \frac{(-s)^l \mu^{l+\text{m}} (2\pi k)^{4(l+\text{m})}}{l!} \left[\text{Im} \left(e^{2i\pi k \frac{t}{n}} \right) + O\left(\frac{k}{n} \right) \right] ds$$

$$+ \sum_{k=1}^{M} \frac{\beta_k}{(\text{m}-1)!} \int_0^\infty e^{-s} s^{\text{m}-1} \sum_{l=0}^{\infty} \frac{(-s)^l \mu^{l+\text{m}} (2\pi k)^{4(l+\text{m})}}{l!} \left[\text{Re} \left(e^{2i\pi k \frac{t}{n}} \right) + O\left(\frac{k}{n} \right) \right] ds$$

$$= \sum_{k=1}^{M} \frac{\alpha_k \{\mu(2\pi k)^4\}^{\text{m}}}{(\text{m}-1)!} \left[\text{Im} \left(e^{2i\pi k \frac{t}{n}} \right) + O\left(\frac{k}{n} \right) \right] \int_0^\infty e^{-s - s\mu(2\pi k)^4} s^{\text{m}-1} ds$$

$$+ \sum_{k=1}^{M} \frac{\beta_k \{\mu(2\pi k)^4\}^{\text{m}}}{(\text{m}-1)!} \left[\text{Re} \left(e^{2i\pi k \frac{t}{n}} \right) + O\left(\frac{k}{n} \right) \right] \int_0^\infty e^{-s - s\mu(2\pi k)^4} s^{\text{m}-1} ds$$

$$= \sum_{k=1}^{M} \frac{\alpha_k \{\mu(2\pi k)^4\}^{\text{m}}}{(1+\mu(2\pi k)^4)^{\text{m}}} \left[\text{Im} \left(e^{2i\pi k \frac{t}{n}} \right) + O\left(\frac{k}{n} \right) \right]$$

$$+ \sum_{k=1}^{M} \frac{\beta_k \{\mu(2\pi k)^4\}^{\text{m}}}{(1+\mu(2\pi k)^4)^{\text{m}}} \left[\text{Re} \left(e^{2i\pi k \frac{t}{n}} \right) + O\left(\frac{k}{n} \right) \right]$$

$$= \sum_{k=1}^{M} \frac{\{\mu(2\pi k)^4\}^{\text{m}}}{(1+\mu(2\pi k)^4)^{\text{m}}} \left[\alpha_k \text{Im} \left(e^{2i\pi k \frac{t}{n}} \right) + \beta_k \text{Re} \left(e^{2i\pi k \frac{t}{n}} \right) \right]$$

$$+ \sum_{k=1}^{M} \frac{\{\mu(2\pi k)^4\}^{\text{m}}}{(1+\mu(2\pi k)^4)^{\text{m}}} (\alpha_k + \beta_k) O\left(\frac{M}{n} \right).$$

We assume $\max_k \{\alpha_k, \beta_k\} < \infty$. Hence,

$$\sum_{k=1}^{M} \frac{\{\mu(2\pi k)^4\}^{\text{m}}}{(1+\mu(2\pi k)^4)^{\text{m}}} (\alpha_k + \beta_k) O\left(\frac{M}{n} \right) = O\left(\frac{M}{n} \right) \sum_{k=1}^{M} (\alpha_k + \beta_k)$$

$$= O\left(\frac{M}{n}\right) M \max_k \{\alpha_k, \beta_k\}$$

$$= O\left(\frac{M^2}{n}\right).$$

Therefore,

$$(1 - S_n^\lambda)^{\mathrm{m}} g\left(\frac{t}{n}\right) = \sum_{k=1}^{M} \frac{\{\mu(2\pi k)^4\}^{\mathrm{m}}}{(1 + \mu(2\pi k)^4)^{\mathrm{m}}} \left[\alpha_k \mathrm{Im}\left(e^{2i\pi k \frac{t}{n}}\right) + \beta_k \mathrm{Re}\left(e^{2i\pi k \frac{t}{n}}\right)\right] + O\left(\frac{M^2}{n}\right). \quad (73)$$

The desired result (69) follows if we can show that the summation in (73) tends to 0. Note that $\left|e^{2i\pi k \frac{t}{n}}\right| < 1$ and hence the summations will go to zero if $\left(\frac{\mu(2\pi k)^4}{1 + \mu(2\pi k)^4}\right)^{\mathrm{m}} \to 0$ for all k. As shown in the proof of Theorem 4.1, $\left(\frac{\mu k^4}{1 + \mu k^4}\right)^{\mathrm{m}}$ goes to zero if $\frac{M^4}{\mathrm{m}} \to 0$, where $k \leq M$. Thus $\left(1 - S_n^\lambda\right)^m \frac{g_n\left(\frac{t}{n}\right)}{n^H} \to 0$ combined with the results of Theorem 4.1 imply

$$(1 - (1 - S_n^\lambda)^{\mathrm{m}})\frac{y_{\lfloor nr \rfloor}}{n^H} = \frac{\hat{f}^{\mathrm{m}}_{\lfloor nr \rfloor}}{n^H} \to g(r) + B_H(r),$$

almost surely as $n \to \infty$ and $\mathrm{m} \to \infty$ and this completes the proof.

Proof of Proposition 4.5: The proof is similar to the proof of the corresponding result for the Brownian motion case in (Phillips and Shi, 2021, Theorem 2) and is omitted.

Proof of Theorem 4.6: We have $(1 - (1 - S_n^\lambda)^{\mathrm{m}})\frac{y_{\lfloor nr \rfloor}}{n^H} = (1 - (1 - S_n^\lambda)^{\mathrm{m}})\left[\frac{g_n(\lfloor nr \rfloor)}{n^H} + \frac{x_{\lfloor nr \rfloor}}{n^H}\right]$. It is already shown in Theorem 4.1 that $(1 - (1 - S_n^\lambda)^{\mathrm{m}})\frac{x_{t=\lfloor nr \rfloor}}{n^H} \xrightarrow{a.s} B_H(r)$. Hence it remains to show that $(1 - (1 - S_n^\lambda)^{\mathrm{m}})\frac{g_{\lfloor nr \rfloor}}{n^H} = g(r)$ as $n \to \infty$. Recall that $\frac{g_{\lfloor nr \rfloor}}{n^H} \to g(r)$ for all $r \in [0,1]$. By the Weierstrass approximation theorem, for any $\epsilon > 0$, there exists some $p \in \mathcal{N}$ such that $|P(r) - g(r)| < \epsilon$ for all $r \in [0,1]$, where $P(\cdot)$ is a p'th degree polynomial. On the other hand, $(1 - (1 - S_n^\lambda)^{\mathrm{m}})\frac{g_n(\lfloor nr \rfloor)}{n^H} = (1 - (1 - S_n^\lambda)^{\mathrm{m}}g(r) + o(1)$, which implies $\left|(1 - (1 - S_n^\lambda)^{\mathrm{m}})\left(\frac{g_{\lfloor nr \rfloor}}{n^H} - P(r)\right)\right| < \epsilon + o(1)$. Now, by following the proof of Proposition 4.5 we can show $(1 - (1 - S_n^\lambda)^{\mathrm{m}})P(\frac{t=\lfloor nr \rfloor}{n}) \to P(r)$ where as $n, m \to \infty$. Thus given any $\epsilon > 0$, there exists a p'th degree polynomial such that $\left|(1 - (1 - S_n^\lambda)^{\mathrm{m}})\frac{g_{\lfloor nr \rfloor}}{n^H} - P(r)\right| < \epsilon$ as $n, m \to \infty$. This completes the proof.

Proof of Proposition 4.7: The proof is similar to the proof of Phillips and Shi (2021, Theorem 3) when $g(r)$ is piecewise polynomial and is omitted. Next, let $g(\cdot)$ be of the form (40). Define $r_0 = 0$ and $r_{b+1} = 1$. Now, by imitating the proof of Proposition 4.4, we find $\frac{\hat{f}^{\mathrm{m}}_{\lfloor nr \rfloor}}{n^H} \xrightarrow{a.s.} g(r) + B_H(r)$ for $r \in (r_i, r_{i+1})$, where $i = 0, 1, \cdots, b$. Thus at points of continuity $\frac{\hat{f}^{\mathrm{m}}_{\lfloor nr \rfloor}}{n^H} \xrightarrow{a.s.} g(r) + B_H(r)$. For $r = r_i, i = 1, 2, \cdots, b$, we consider two intervals $[r_{i-1}, r_i)$ and $[r_i, r_{i+1})$. Now $g(r)$ has finite left and right limit at $r = r_i$ and fBm is a continuous process. Hence,

$$\lim_{r \to r_i-} \frac{\hat{f}^{\mathrm{m}}_{\lfloor nr \rfloor}}{n^H} = \lim_{r \to r_i-} g(r) + B_H(r_i) \quad \text{and} \quad \lim_{r \to r_i+} \frac{\hat{f}^{\mathrm{m}}_{\lfloor nr \rfloor}}{n^H} = \lim_{r \to r_i+} g(r) + B_H(r_i).$$

On the other hand, the bHP filter evaluated at any interior point $r \in (0,1)$ employs the neighboring data points on both left and right sides symmetrically for sufficiently large n. Therefore, at any breakpoint $\{r_i\}_{i=1}^b$,

$$\frac{\hat{f}_{\lfloor nr \rfloor}^{\mathrm{m}}}{n^H} \xrightarrow{a.s.} \frac{1}{2} \left[\lim_{r \to r_i-} g(r) + \lim_{r \to r_i+} g(r) \right] + B_H(r_i)$$

and this completes the proof.

Proof of Theorem 4.8: Let $g(\cdot)$ take the following form

$$g(r) = \begin{cases} g_1(r) & r \in [r_0, r_1) \text{ where } r_0 = 0 \\ g_2(r) & r \in [r_1, r_2) \\ \vdots & \vdots \\ g_{b+1}(r) & r \in [r_b, r_{b+1}] \text{ where } r_{b+1} = 1. \end{cases}$$

Each g_i is bounded continuous and hence $g(\cdot)$ has bounded left and right limits at all break points. Consider g_i on the interval $[r_{i-1}, r_i]$, where $i = 1, 2, ..., b+1$. By the Weierstrass approximation given $\epsilon > 0$ we can find a polynomial P_i of order p_i, such that $|P_i(r) - g_i(r)| < \epsilon$ for all $r \in [r_{i-1}, r_i]$. Thus for a fixed $\epsilon > 0$, we obtain $b + 1$ many polynomials $\{P_i\}_{i=1}^{b+1}$ with order $\{p_i\}_{i=1}^{b+1}$ such that $|P_i(r) - g_i(r)| < \epsilon$ for $r \in [r_{i-1}, r_i)$. Using Proposition 4.7 gives the required result.

8 Appendix B: Strong Approximation

Lemma 2.2 in the main text gives a strong approximation for fBM with Hurst parameter $H \in (1/2, 1)$. To extend the domain of strong approximation to $H \in (0, 1)$ we briefly outline the approach developed by Szabados (2001) who constructed a stochastic process that converges to fBM with $H \in (0, 1)$ using simple moving averages of a random walk. The so-called KMT approximation (Komlós et al., 1976) is used in this development and the result is given as follows.

Suppose the sequence of random variables $\{X_t\} \sim iid(0, 1)$ has finite moment generating function $\mathbb{E}(\exp(uX_1)) < \infty$ for $|u| \le u_0$, where $u_0 > 0$ and for which the partial sums $S(k) = X_1 + \cdots + X_k$ for $k > 0$ are as close to BM as possible. If $\{W(t)\}_{t \ge 0}$ is a given Wiener process, then for any $n \ge 1$ a sequence $W(1), \cdots, W(N)$ can be constructed, such that the following holds (Komlós et al., 1976, theorem 1))

$$P\left(\max_{0 \le k \le N} |S(k) - W(k)| > C_0 \log n + x \right) < K_0 e^{-\bar{\lambda}x},$$

for any $x > 0$, where C_0, K_0 and $\bar{\lambda}$ are positive constants that may depend on the distribution of X_k, but not on N and x.

Using this result Szabados (2001) constructed a new stochastic process based on $S(k)$, that converges to fBM for $H \in (0, 1)$. For any integer $p > 0$, let $\Delta t = 2^{-2p}$ and $t_x = x\Delta t$. He defined a shrunken random walk $B_p^*(t_k) = 2^{-p}S_p(k)$, where $0 \le k \le K2^{2p}$ and $K > 0$. Finally, a new

stochastic process is presented as follows

$$B_p^{*(H)}(t_k) = \sum_{r=-\infty}^{k-1} h(t_r, t_k)[B_p^*(t_r + \Delta t) - B_p^*(t_r)]$$

$$= \frac{2^{-2Hp}}{\Gamma(H + \frac{1}{2})} \sum_{r=-\infty}^{k-1} [(k-r)^{H-\frac{1}{2}} - (-r)_+^{H-\frac{1}{2}}]X_p(r+1),$$

(74)

where $(a)_+ = \max\{0, a\}$ and

$$h(s, t) = \frac{1}{\Gamma(H + \frac{1}{2})}[(k-r)^{H-\frac{1}{2}} - (-r)_+^{H-\frac{1}{2}}], \ \ s \le t.$$

Theorem 8.1. *(Szabados, 2001, theorem 3) For any $H \in (0, 1)$, a sequence of processes $B_p^{*(H)}(t)$ $(t \ge 0, \ p = 0, 1, 2, \cdots)$ can be constructed that converges a.s. and uniformly to a fBM $B^H(t)$ on any compact interval $[0, K]$, $K > 0$. If $p \ge 1$, $C \ge 2$ and C_0 is large enough, it follows that*

$$P\left(\max_{0 \le k \le K} |B^H(t) - B_p^{*(H)(t)}| \ge \frac{\bar{\alpha}^*}{(1 - 2^{-\beta^*(H)})^2}p2^{-\beta^*(H)p}\right) \le 6(K2^{2p})^{1-C} + 4K_o(K2^{2p})^{-\bar{\lambda}C_o}$$

The undefined constants used in this result are given in Szabados (2001) and are not required for the current development.

Now define a stochastic process $D_p^H(t_k) : k = 0, \cdots, 2^{2p}$ for $H \in (0, 1)$ by the following equation.

$$D_p^H(t_k) = \frac{1}{\Gamma(H + \frac{1}{2})} \sum_{r=-\infty}^{k-1} [(k-r)^{H-\frac{1}{2}} - (-r)_+^{H-\frac{1}{2}}]X_p(r+1) = B_p^{*(H)}(t_k)2^{2Hp} \quad (75)$$

As $p \to \infty$, it follows from Theorem 8.1 that for any $H \in (0, 1)$,

$$\frac{D_p^H(t)}{2^{2Hp}} \overset{a.s.}{\to} B_H(t). \quad (76)$$

References

BUJA, A., T. HASTIE, AND R. TIBSHIRANI (1989): "Linear smoothers and additive models," *The Annals of Statistics*, 453–510.

DAVIDSON, J. AND N. HASHIMZADE (2009): "Type I and type II fractional Brownian motions: A reconsideration," *Computational Statistics & Data Analysis*, 53, 2089–2106.

DZHAPARIDZE, K. AND H. VAN ZANTEN (2004): "A series expansion of fractional Brownian motion," *Probability theory and related fields*, 130, 39–55.

GIRAITIS, L., H. L. KOUL, AND D. SURGAILIS (2012): *Large Sample Inference for Long Memory Processes*, London: Imperial College Press.

HALL, V. B. AND P. THOMSON (2021): "Does Hamilton's OLS regression provide a better alternative to the Hodrick-Prescott filter? A New Zealand business cycle perspective," *Journal of Business Cycle Research*, 17(2), 151–183.

HALL, V. B. AND P. THOMSON (2022): "A boosted HP filter for New Zealand business cycle analysis," *Victoria University of Wellington, Working Paper*, 1/2022.

HAMILTON, JAMES, D. (2018): "Why you should never use the Hodrick-Prescott filter," *Review of Economics and Statistics*, 831–843.

HAMILTON, JAMES, D. (2022): "Dates of U.S. recessions as inferred by GDP-based recession indicator, retrieved from FRED, Federal Reserve Bank of St. Louis;" https://fred.stlouisfed.org/series/JHDUSRGDPBR.

HODRICK, ROBERT, J. AND E. C. PRESCOTT (1980): "Post-War US Business Cycles: An Empirical Investigation," *DiscussionPaper 451. Evanston, 11: Center for Mathematical Studies in Economics and Management Science, Northwestern University*.

HODRICK, R. J. AND E. C. PRESCOTT (1997): "Postwar US business cycles: an empirical investigation," *Journal of Money, credit, and Banking*, 1–16.

KIM, S.-J., K. KOH, S. BOYD, AND D. GORINEVSKY (2009): "ℓ_1 trend filtering," *SIAM review*, 51, 339–360.

KOMLÓS, J., P. MAJOR, AND G. TUSNÁDY (1976): "An approximation of partial sums of independent RV's, and the sample DF. II," *Zeitschrift für Wahrscheinlichkeitstheorie und verwandte Gebiete*, 34, 33–58.

LESER, C. E. V. (1961): "A simple method of trend construction," *Journal of the Royal Statistical Society: Series B (Methodological)*, 23, 91–107.

MARINUCCI, D. AND P. M. ROBINSON (1999): "Alternative forms of fractional Brownian motion," *Journal of statistical planning and inference*, 80, 111–122.

MCELROY, T. (2008): "Exact formulas for the Hodrick-Prescott filter," *Econometrics Journal*, 11, 1–9.

MEI, Z., P. C. B. PHILLIPS AND Z. SHI (2022): "The boosted HP filter is more general than you might think," *Working Paper, Yale University*.

PHILLIPS, P. C. B. AND S. JIN (2021): "Business cycles, trend elimination, and the HP filter," *International Economic Review*, 62, 469–520.

PHILLIPS, P. C. B. (2022): "Discrete Fourier transforms of fractional processes with econometric applications", *Advances in Econometrics* (forthcoming).

PHILLIPS, P. C. B. AND S. JIN (2002): "Limit behavior of the Whittaker (HP) filter," *Working Paper, Yale University*.

PHILLIPS, P. C. B. AND Z. SHI (2021): "Boosting: Why you can use the Hodrick-Prescott filter," *International Economic Review*, 62, 521–570.

SHIMOTSU, K. AND P. C. B. PHILLIPS (2005): "Exact local Whittle estimation of fractional integration," *The Annals of Statistics*, 33, 1890–1933.

SZABADOS, T. (2001): "Strong approximation of fractional Brownian motion by moving averages of simple random walks," *Stochastic processes and their applications*, 92, 31–60.

TAQQU, M. AND G. SAMORODNITSKY (1996): *Stable Non-Gaussian Random Processes: Stochastic Models with Infinite Variance*, Chapman and Hall.

TIBSHIRANI, R. J. (2014): "Adaptive piecewise polynomial estimation via trend filtering," *Annals of statistics*, 42, 285–323.

TUKEY, J. W. (1977): *Exploratory data analysis*, vol. 2, Reading, MA.

VAN DER VAART, A. AND J. WELLNER (1996): *Weak convergence and empirical processes: with applications to statistics*, Springer-Verlag, New York.

WANG, Q., LIN, YAN-XIA, AND C. M. GULATI (2003): "Strong Approximation for Long Memory Processes with Applications," *Journal of Theoretical Probability*, 377–389.

WHITTAKER, E. T. (1922): "On a new method of graduation," *Proceedings of the Edinburgh Mathematical Society*, 41, 63–75.

WHITTAKER, E. T. AND G. ROBINSON (1924): *The Calculus of Observations: a Treatise on Numerical Mathematics*.

YAMADA, H. AND R. BAO (2021): "ℓ_1 Common Trend Filtering," *Computational Economics*.